



**TRIBHUVAN UNIVERSITY  
INSTITUTE OF ENGINEERING  
PULCHOWK CAMPUS**

**Thesis No.: PUL080MSMSE010**

**HYDROTHERMAL SYNTHESIS OF CARBON QUANTUM DOTS  
FROM MANGO PEEL WASTE AND THEIR APPLICATION IN  
PHOTOCATALYTIC DEGRADATION OF METHYLENE BLUE**

**BY**

**NIKITA SHRESTHA**

**A THESIS**

**SUBMITTED TO THE DEPARTMENT OF APPLIED SCIENCE AND  
CHEMICAL ENGINEERING**

**IN PARTIAL FULFILLMENT OF THE REQUIREMENTS FOR THE DEGREE  
OF MASTER OF SCIENCE IN MATERIAL SCIENCE AND ENGINEERING**

**DEPARTMENT OF APPLIED SCIENCE AND CHEMICAL ENGINEERING  
LALITPUR, NEPAL**

**MAY, 2026**

# Declaration

I hereby declare that this study/research entitled **Hydrothermal Synthesis of Carbon Quantum Dots from Mango Peel Waste and Their Application in Photocatalytic Degradation of Methylene Blue** is based on our original research work. Related works on the topic by other researchers have been duly acknowledged. I owe all the liabilities relating to the accuracy and authenticity of the data and any other information included here under.

**Nikita Shrestha ( 080MSMSE010)**

Date: 15-05-2026

# Recommendation

This is to certify that this project report entitled **Hydrothermal Synthesis of Carbon Quantum Dots from Mango Peel Waste and Their Application in Photocatalytic Degradation of Methylene Blue** prepared and submitted by **Nikita Shrestha & 080MSMSE010**, in partial fulfillment of the requirements of the Master degree of Engineering in Material Science and Engineering, awarded by Tribhuvan University, has been completed under my supervision. I recommend the same for acceptance by Tribhuvan University.

---

Name of the Supervisor: Asst. Prof. Dr. Khem Raj Shrestha

Designation: Assistant Professor

Organization: Pulchowk Campus

Date: 15-05-2026

# Letter of Approval

TRIBHUVAN UNIVERSITY  
INSTITUTE OF ENGINEERING  
PULCHOWK CAMPUS  
DEPARTMENT OF APPLIED SCIENCE AND CHEMICAL ENGINEERING

This project/thesis entitled **Hydrothermal Synthesis of Carbon Quantum Dots from Mango Peel Waste and Their Application in Photocatalytic Degradation of Methylene Blue** prepared and submitted by **Nikita Shrestha 080MSMSE010** has been examined by us and is accepted for the award of the Master's degree in Material Science and Chemical engineering.

.....  
**Asst. Prof. Dr. Khem Raj Shrestha**

Supervisor

Department of Applied Science and  
Chemical Engineering  
Pulchowk Campus, Institute of Engineering  
Tribhuvan University, Nepal

.....  
**Prof. Dr. Armila Rajbhandari  
(Nyachhyon)**

External Examiner

Central Department of Chemistry, TU  
Kirtipur, Kathmandu, Nepal

.....  
**Prof. Dr. Sahira Joshi**

Head of Department

Department of Applied Science and  
Chemical Engineering Pulchowk Campus, Institute of Engineering  
Tribhuvan University, Nepal

Date of approval: 15-05-2026

# Copyright

The author has agreed that the Library, Department of Material Science and Chemical Engineering, Pulchowk Campus, and Institute of Engineering may make this report available for inspection. Moreover, the author has agreed that permission for extensive copying of this project report for scholarly purposes may be granted by the supervisors who supervised the work recorded herein or, in their absence, by the Head of the Department wherein the project report was done. It is understood that recognition will be given to the author of this report and the Department of Applied Science and Chemical Engineering, Pulchowk Campus, Institute of Engineering for any use of the material of this project report. Copying publication or the other use of this report for financial gain without the approval of the Department of Applied Science and Chemical Engineering, Pulchowk Campus, Institute of Engineering, and the author's written permission is prohibited.

Request for permission to copy or to make any other use of the material in this report in whole or in part should be addressed to:

Head

Department of Applied Science and Chemical Engineering

Pulchowk Campus, Institute of Engineering, TU

Lalitpur, Nepal.

# Acknowledgments

I express my sincere gratitude to the Department of Applied Science and Chemical Engineering, Pulchowk Campus, Tribhuvan University, for providing access to the laboratory facilities necessary for the successful completion of this research.

I would like to extend my heartfelt thanks to my supervisor, Asst. Prof. Dr. Khem Raj Shrestha, for his invaluable guidance, continuous support, and encouragement throughout this study. His insightful suggestions and constructive feedback significantly enhanced the quality of this work and helped me overcome various challenges during the research process. His mentorship has inspired me to approach research with dedication, discipline, and critical thinking. I would also like to express my sincere appreciation to Prof. Chhabi Lal Gnawali for his valuable guidance and support during this research work. I would also like to acknowledge ASCOL Campus for their support in conducting the FTIR analysis, which contributed significantly to the characterization part of this study. I would also like to express my heartfelt gratitude to the Department of Mechanical Engineering, Aristotle University of Thessaloniki (AUTH), Greece, for providing laboratory access, research facilities, and a valuable academic environment during the course of this study. The opportunity to conduct part of this research work in an international research setting greatly enhanced my learning experience and research exposure.

Finally, I would like to thank everyone who directly or indirectly supported me in completing this research successfully.

**Nikita Shrestha (080MSMSE010)**

# Abstract

Carbon quantum dots (CQDs) are promising nanomaterials due to their excellent fluorescent properties, low toxicity, and environmental compatibility. In this research, CQDs were synthesized from mango peel waste using a simple and eco-friendly hydrothermal method. The synthesized CQDs were characterized using UV–Visible spectroscopy and fluorescence analysis, that showed strong blue and green fluorescence under 254 nm and 365 nm UV light, confirming their successful formation. The CQDs showed UV absorption mainly between 200-290 nm, indicating the presence of carbon core structures and oxygen-containing functional groups. For photocatalytic studies, firstly the initial absorbance of methylene blue (MB) solution was measured, then followed by analysis of samples after exposure to CQDs under UV light and sunlight. The MB dye solution containing CQDs was irradiated for 15, 30, 60, and 90 minutes under both conditions. Degradation percentage was calculated based on the difference in absorbance values. Under both circumstances, the degradation efficiency improved with the irradiation time. The degradation efficiency reached 67.83 % under UV light and 26.84% under sunlight after 90 minutes, showing improved efficiency under UV irradiation. This improved performance under UV irradiation is explained by increased production of reactive species that cause dye degradation and more effective excitation of CQDs. Fourier Transform Infrared (FTIR) spectroscopy, Fluorescence analysis, and UV-Visible spectroscopy were used to analyze the produced CQDs. The presence of hydroxyl groups (–OH), C=O, and C–O functional groups on the CQDs surface, which are beneficial for adsorption and photocatalytic activity, was confirmed by FTIR findings.

Thus, the study shows that CQDs made from mango peels are an economical, sustainable, and effective material for photocatalytic degradation with great promise for wastewater treatment and environmental remediation applications.

Keywords: *Green Synthesis, UV–Vis Spectroscopy, Fluorescence, Wastewater remediation*

# Contents

<b>Declaration</b>	<b>i</b>
<b>Recommendation</b>	<b>ii</b>
<b>Page of Approval</b>	<b>iii</b>
<b>Copyright</b>	<b>iv</b>
<b>Acknowledgements</b>	<b>v</b>
<b>Abstract</b>	<b>vi</b>
<b>Contents</b>	<b>x</b>
<b>List of Figures</b>	<b>xi</b>
<b>List of Tables</b>	<b>xii</b>
<b>List of Abbreviations</b>	<b>xiii</b>
<b>List of Units and conversions</b>	<b>xiv</b>
<b>1 Introduction</b>	<b>1</b>
1.1 Background . . . . .	1
1.2 Statement of the Problem . . . . .	4
1.3 Scope and Limitations . . . . .	5
1.4 Research Objectives . . . . .	6
1.5 Significance/Rationale of the Study . . . . .	6
1.5.1 Environmental Significance . . . . .	7
1.5.2 Environmental Significance . . . . .	7
1.5.3 Scientific Significance . . . . .	8
1.5.4 Economic and Sociotechnical Significance . . . . .	8
1.5.5 Contribution to the Local Research Landscape . . . . .	8

<b>2</b>	<b>Literature Review</b>	<b>10</b>
2.1	Introduction to Carbon Quantum Dots . . . . .	10
2.2	Synthesis of Carbon Quantum Dots . . . . .	10
2.2.1	Top-Down Approaches . . . . .	10
2.2.2	Bottom-Up Approaches . . . . .	11
2.2.3	Hydrothermal Synthesis . . . . .	11
2.2.4	Pyrolysis . . . . .	12
2.2.5	Microwave-Assisted Synthesis . . . . .	12
2.2.6	Biomass-Derived CQDs . . . . .	13
2.3	Characterization of Carbon Quantum Dots . . . . .	14
2.4	Applications in Environmental Remediation and Sensing . . . . .	16
2.4.1	Metal Ion Sensing . . . . .	16
2.4.2	Photocatalytic Degradation . . . . .	16
2.4.3	UV vs Sunlight Photocatalysis . . . . .	17
2.5	Research Gap and Justification . . . . .	17
2.5.1	Research Gap . . . . .	17
2.5.2	Justification of the Study . . . . .	18
<b>3</b>	<b>Methodology</b>	<b>19</b>
3.1	Materials . . . . .	19
3.1.1	Source of Raw Material . . . . .	19
3.1.2	Chemicals and Reagent . . . . .	19
3.2	Synthesis of Carbon Quantum Dots from Mango Peel . . . . .	19
3.2.1	Raw Material Preparation . . . . .	19
3.2.2	Hydrothermal Synthesis of CQDs . . . . .	20
3.2.3	Preparation of the Precursor Suspension . . . . .	20
3.2.4	Hydrothermal Carbonisation . . . . .	21
3.3	Photocatalytic Degradation of Methylene Blue using Mango Peel CQDs . . . . .	21
3.3.1	Methylene Blue Solution Preparation . . . . .	21
3.3.2	Adsorption–Desorption Equilibrium Study . . . . .	21
3.3.3	Photocatalytic Reaction . . . . .	21
3.3.4	Sampling and Analysis . . . . .	22
3.3.5	Degradation Efficiency Calculation . . . . .	22
3.4	Purification of the CQD Suspension . . . . .	22
3.5	Characterisation of the Synthesised CQDs . . . . .	22
3.5.1	UV–Visible Absorption Spectroscopy . . . . .	22

3.5.2	Photoluminescence (Fluorescence) Analysis . . . . .	23
3.5.3	Fourier Transform Infrared (FTIR) Spectroscopy . . . . .	23
3.6	Photocatalytic Degradation of Methylene Blue . . . . .	24
3.6.1	Preparation of Methylene Blue Solution . . . . .	24
3.6.2	Dark Adsorption Equilibration . . . . .	24
3.6.3	Light Irradiation Setup . . . . .	24
3.6.4	Sample Collection and Analysis . . . . .	24
3.7	Degradation Efficiency Calculation . . . . .	25
3.8	Data Analysis and Graphical Representation . . . . .	25
<b>4</b>	<b>Results &amp; Discussion</b>	<b>26</b>
4.1	Hydrothermal Synthesis Mechanism . . . . .	26
4.2	Photocatalytic Degradation Mechanism of Methylene Blue (MB) . . . . .	27
4.3	Visual Appearance and Fluorescence Properties . . . . .	27
4.4	UV-Vis Spectroscopic Characterization . . . . .	28
4.5	FTIR Characterization . . . . .	30
4.6	Adsorption Behavior of Methylene Blue under Dark Conditions . . . . .	32
4.7	Photocatalytic Degradation of Methylene Blue under UV Light . . . . .	32
4.8	Photocatalytic Degradation of Methylene Blue under Sunlight . . . . .	34
4.9	Comparative Analysis: UV Light versus Sunlight . . . . .	34
4.10	UV-Vis absorbance spectra of methylene blue (10 mg/L) degradation over time in the presence of mango peel-derived CQDs at $\lambda = 664$ nm . . . . .	35
4.11	Effect of Irradiation Time on Absorbance of Methylene Blue under UV Light and Sunlight . . . . .	37
4.12	Comparative Kinetic Behavior of Methylene Blue Degradation in the Presence of Mango Peel-Derived CQDs under UV Irradiation and Sunlight . . . . .	37
4.13	Effect of Irradiation Time on Degradation efficiency of Methylene Blue under UV Light and Sunlight . . . . .	38
<b>5</b>	<b>Conclusion</b>	<b>40</b>
<b>6</b>	<b>Limitations and Future enhancement</b>	<b>42</b>
6.1	Limitations . . . . .	42
6.2	Future Enhancement . . . . .	42
	<b>References</b>	<b>43</b>

<b>Appendices</b>	<b>50</b>
Appendix . . . . .	51
Appendix A: Raw Experimental Data . . . . .	51
Appendix B: UV-Vis Spectral Peak Summary . . . . .	52
Appendix C: FTIR Peak Assignments . . . . .	52
Appendix D: Sample Degradation Efficiency Calculation . . . . .	53
Appendix E: Kinetic Analysis Data . . . . .	54

# List of Figures

1.1	Diagrammatic representation of the Hydrothermal process (Mehta VN, Kailasa SK. 2021) . . . . .	3
1.2	fig:Application of CQD (Lei Ye, Kaustubh Naik, 2022) . . . . .	3
1.3	fig:Application of CQD (Lei Ye, Kaustubh Naik, 2022) . . . . .	4
3.1	Diagrammatic representation of the preparation of raw material . . . . .	20
3.2	Diagrammatic representation of the Hydrothermal process . . . . .	21
4.1	Testing of the sample in the UV chamber . . . . .	28
4.2	Testing of Undiluted sample in the UVA 365nm lamp . . . . .	28
4.3	Testing of Ethanol diluted sample in the UVA 365nm lamp . . . . .	29
4.4	Testing of Distilled water diluted sample in the UVA 365nm lamp . . . . .	29
4.5	Normal (Undiluted Sample) . . . . .	29
4.6	Ethanol Diluted Sample . . . . .	30
4.7	Distilled Water Sample . . . . .	30
4.8	FTIR spectrum of carbon quantum dots (CQDs) synthesized from mango peel via hydrothermal treatment. . . . .	31
4.9	Photocatalytic degradation of methylene blue under UV ( $A_0 = 1.315$ , $\lambda = 664$ nm) . . . . .	33
4.10	Photocatalytic degradation of methylene blue under Sunlight ( $A_0 = 1.315$ , $\lambda = 664$ nm) . . . . .	35
4.11	(a) UV light . . . . .	36
4.12	(b) Sunlight . . . . .	36
4.13	Variation of methylene blue absorbance with irradiation time in the presence of CQDs under UV light and sunlight. . . . .	37
4.14	Comparison of methylene blue degradation kinetics under UV light and sunlight using $\ln\left(\frac{A_0}{A_t}\right)$ versus time.. . . .	38
4.15	Degradation efficiency of methylene blue under UV light and sunlight with irradiation time. . . . .	39

# List of Tables

4.1	Adsorption Behaviour of Methylene Blue in the Presence of CQDs under Dark Conditions ( $A_0 = 1.315$ , $\lambda = 664\text{nm}$ ) . . . . .	32
4.2	Photocatalytic degradation of methylene blue under UV irradiation ( $A_0 = 1.315$ , $\lambda = 664\text{nm}$ ) . . . . .	33
4.3	Photocatalytic degradation of methylene blue under Sunlight irradiation ( $A_0 = 1.315$ , $\lambda = 664\text{ nm}$ ) . . . . .	34
4.4	Comparative Degradation Efficiency: UV Light vs. Sunlight Irradiation ( $A_0 = 1.315$ , $\lambda = 664\text{ nm}$ ) . . . . .	35
6.1	Raw absorbance data for MB adsorption under dark conditions ( $A_0 = 1.315$ , $\lambda = 664\text{ nm}$ ) . . . . .	51
6.2	Raw absorbance data for MB degradation under UV irradiation ( $A_0 = 1.315$ , $\lambda = 664\text{ nm}$ ) . . . . .	51
6.3	Raw absorbance data for MB degradation under sunlight ( $A_0 = 1.315$ , $\lambda = 664\text{ nm}$ )	52
6.4	Summary of UV-Vis spectral features of CQDs under different solvent conditions .	52
6.5	FTIR absorption peaks and their assignments for mango peel-derived CQDs . . . .	52
6.6	Calculated $\ln(A_0/A_t)$ values for MB degradation under UV and sunlight . . . . .	54

# List of Abbreviations

<b>CQDs</b>	Carbon Quantum Dots
<b>MB</b>	Methylene Blue
<b>UV</b>	Ultraviolet
<b>FTIR</b>	Fourier Transform Infrared Spectroscopy
<b>UV-Vis</b>	Ultraviolet-Visible Spectroscopy
<b>ROS</b>	Reactive Oxygen Species
<b>TEM</b>	Transmission Electron Microscopy
<b>XRD</b>	X-Ray Diffraction
<b>SEM</b>	Scanning Electron Microscopy
<b>MPP</b>	Mango Peel Powder
<b>PL</b>	Photoluminescence
<b>AOPs</b>	Advanced Oxidation Processes
<b>rGO</b>	Reduced Graphene Oxide
<b>OH</b>	Hydroxyl Group
<b>COOH</b>	Carboxyl Group
<b>rpm</b>	Revolutions Per Minute
<b>IOE</b>	Institute of Engineering
<b>TU</b>	Tribhuvan University
<b>UVA</b>	Ultraviolet A

# List of units and conversions

<b>nm</b>	Nanometer (1 nm = $10^{-9}$ m)
<b>cm<sup>-1</sup></b>	Wavenumber
<b>mg/L</b>	Milligram per Liter (concentration unit)
<b>mL</b>	Milliliter (1 mL = $10^{-3}$ L)
<b>g</b>	Gram (1 g = $10^{-3}$ kg)
<b>°C</b>	Degree Celsius
<b>rpm</b>	Revolutions Per Minute
<b>h</b>	Hour (1 h = 60 min = 3600 s)
<b>min</b>	Minute (1 min = 60 s)
$\lambda$	Wavelength (nm)
<b>A<sub>0</sub></b>	Initial Absorbance (dimensionless)
<b>A<sub>t</sub></b>	Absorbance at time $t$ (dimensionless)
$\eta$	Degradation Efficiency (%)

# 1. Introduction

## 1.1 Background

The development of carbon nanomaterials has played an important role in material sciences in the last few decades. With the introduction of graphene, carbon nanotubes, and fullerenes, tremendous breakthroughs have been achieved for various applications from electronics to environment-related areas [1]. Carbon quantum dots (CQDs), which are typically less than 10 nm and can be thought of as zero-dimensional carbon nanomaterials, have recently received attention in scientific research because of their remarkable qualities [2].

Carbon quantum dots (CQDs), which are typically smaller than 10 nm and can be thought of as zero-dimensional carbon nanomaterials, have gained popularity recently. They have exceptional optical properties, including intense photoluminescence, as well as high aqueous solubility, low toxicity, and chemical stability. Because of their remarkable qualities, these characteristics make them perfect candidates for bioimaging, sensing, photocatalysis, and water purification procedures that are prevalent in scientific research [2, 3]. Because they are non-toxic, CQDs are not hazardous to the environment like conventional semiconductor quantum dots, which are frequently made of dangerous heavy metal ions [4].

Recently, there has been interest in the green synthesis of CQDs using renewable biorenewable biomass sources. Due to their availability and environmental sustainability, waste agricultural products including peel fruits and lignocellulosic biomass have been investigated for possible uses. Because of the high bioavailability of its constituents, mango peel (from the plant species known as *Mangifera indica*) can be regarded as a great source of CQDs.

Mango peels make up 7–24% of the total mass of mangoes and are frequently regarded as agro-waste because they are thrown away after processing. Gallotannins, gallic acid, quercetin, carotenoids, and other phenolic compounds that serve as a possible supply of carbon for CQD formation are among the beneficial organic compounds found in mango peel waste [5]. This kind of biomass waste can be used to create useful nanomaterials, which is an inventive "waste to wealth" approach in green chemistry [6, 7].

Hydrothermal synthesis is one of the most popular methods for producing CQDs from biomass because of its ease of use, affordability, and capacity to yield high-quality nanomaterials. The process of carbonizing and transforming organic compounds in an aqueous environment at a specific temperature and pressure is known as hydrothermal synthesis. The resulting CQDs typically include a carbon core with  $sp^2/sp^3$  hybridized regions and surface functional groups like hydroxyl ( $-OH$ ),

carboxyl ( $-\text{COOH}$ ), and carbonyl ( $\text{C}=\text{O}$ ) groups [8].

One significant problem with environmental pollution is the contamination of water bodies by dye contaminants. Water bodies receive dye-polluted wastewater from the textile, leather, and cosmetics industries [9]. One of the most often used dyes is methylene blue (MB). It is said to be hazardous to humans and aquatic life, poisonous, and non-biodegradable [9]. Hence, effective strategies for dye-polluted effluents are imperative.

The use of photocatalytic degradation for breaking down organic pollutants into simple forms has gained momentum due to its ability to decompose pollutants using light energy. Photocatalysis falls within advanced oxidation processes (AOPs), through which pollutants can be degraded into their simplest form without causing secondary contamination [10]. Photocatalysts like  $\text{TiO}_2$  and  $\text{ZnO}$  have been found to show good catalytic efficiency; however, their wide band gap limits their catalytic ability only to the UV part of the electromagnetic spectrum, accounting for less than 5% of solar radiation.

In this regard, the use of carbon nanomaterials, especially CQDs, represents a viable option. CQDs exhibit wide light absorption ranging from UV to visible light, besides having unique photoluminescence property and charge transfer efficiency. The functional group present on the surface of CQDs provides an active site for interaction with pollutants, leading to enhanced adsorption and photocatalysis [2].

Characterization of CQDs is typically carried out using techniques such as UV–Visible spectroscopy, fluorescence spectroscopy, and Fourier Transform Infrared (FTIR) analysis. These methods provide insights into optical properties, electronic transitions, and surface functional groups, which are essential for understanding the behavior and performance of CQDs.

Despite extensive research on CQDs, studies focusing on mango peel-derived CQDs for photocatalytic degradation under different light conditions remain limited. Therefore, the present study aims to synthesize CQDs from mango peel using a hydrothermal method, characterize their physicochemical properties, and evaluate their photocatalytic performance in the degradation of methylene blue under both UV irradiation and natural sunlight.

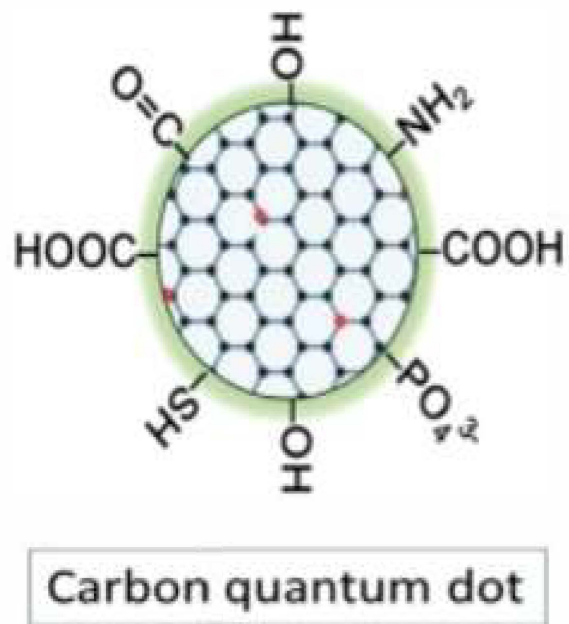


Figure 1.1: Diagrammatic representation of the Hydrothermal process (Mehta VN, Kailasa SK. 2021)

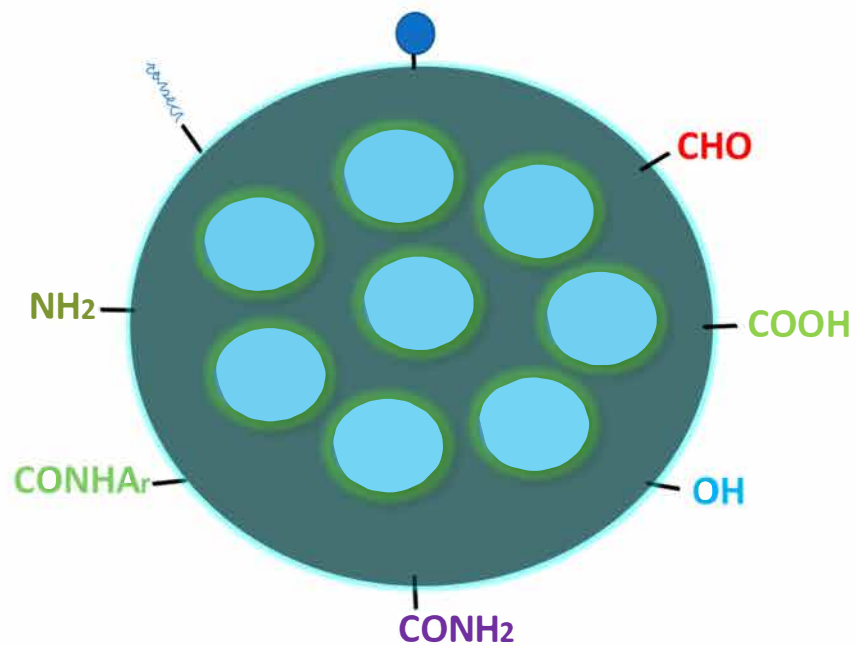


Figure 1.2: Functional Group of CQD (Lei Ye, Kaustubh Naik, 2022)

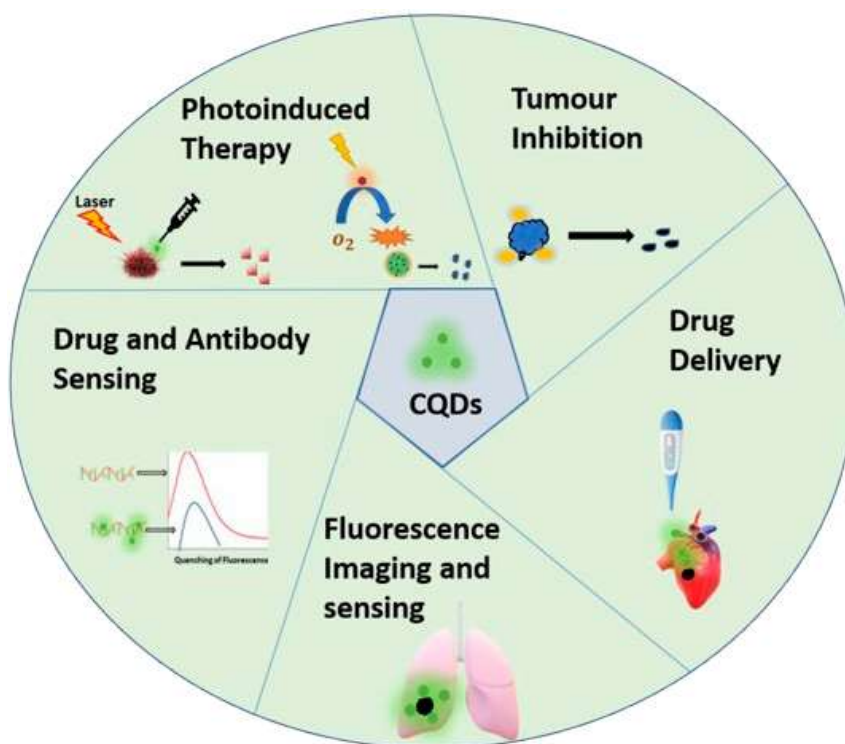


Figure 1.3: Application of CQD (Lei Ye, Kaustubh Naik, 2022)

## 1.2 Statement of the Problem

In recent decades, the pollution of water bodies by synthetic dyes discharged from industries such as textile, leather, cosmetics and pharmaceuticals has emerged as a major environmental problem. It is estimated that the world produces over 700,000 tonnes of dyes annually, of which about 10-15% are released into water bodies during different industrial processes [11]. Among these dyes, methylene blue is one of the most common wastewater contaminants. It is highly soluble, has a stable chemical structure and resistance to natural degradation. Hence, it is difficult to remove by conventional treatment methods [12].

Several treatment techniques have been used to address dye pollution, but each comes with its own limitations. For example, adsorption using activated carbon is effective in removing dyes from water; however, it does not actually eliminate the pollutant but only transfers it to another phase, creating secondary waste that must be managed carefully [13]. Biological treatment methods are good for the environment. They take a long time and do not work well for dyes that do not break down easily. Conventional photocatalysis using materials like TiO<sub>2</sub> can break down dyes quickly. It needs ultraviolet light, which adds to the cost and limits its use on a big scale [14].

In this context carbon quantum dots made from waste biomass have become an option. Mango peel waste, which is produced in amounts and usually thrown away provides a sustainable and

cheap raw material for making these dots. It offers a sustainable and low-cost raw material for CQD synthesis. Although some studies have reported the use of mango peel-derived CQDs for applications such as sensing and bioimaging [15][16], their potential in photocatalytic dye degradation has not been extensively explored. Also there is no comparison between using ultraviolet light and natural sunlight for these applications, which is crucial for understanding how well they work in real life. The use of mango peel-derived carbon quantum dots and natural sunlight could offer a cost- solution for dye degradation. Mango peel waste can be used to make carbon quantum dots which can help in breaking down dyes. Carbon quantum dots, from mango peel can work well with sunlight to degrade dyes [17] [18].

The key issues addressed in this study can be summarized as follows:

- The continuous discharge of methylene blue into water bodies poses significant risks to both the environment and human health, and current treatment methods are not fully effective [19][20].
- Mango peel waste is generated in large amounts and is mostly discarded without any value addition, contributing to environmental pollution [21].
- Conventional photocatalysts such as  $\text{TiO}_2$  and  $\text{ZnO}$  are primarily active under UV light, which represents only a small fraction of the solar spectrum, limiting their efficiency in solar-driven applications [22].
- There is a knowledge vacuum on the practical applicability of mango peel-derived CQDs due to the absence of comparative studies on their performance under UV and natural sunlight. [23].

Thus, this paper deals with the development of environmentally friendly quantum dots from mango peels through the hydrothermal technique as well as the examination of the efficacy of the prepared quantum dots in the degradation of methylene blue dye using UV and natural sunlight.

### **1.3 Scope and Limitations**

#### **Scope**

- Synthesize carbon quantum dots using mango peel via the hydrothermal method.
- Characterize the CQDs using UV–Vis, fluorescence, and FTIR analyses.
- Evaluate the photocatalytic degradation of methylene blue.
- Compare degradation efficiency under UV light and sunlight irradiation.

## **Limitations**

- Limited access to advanced characterization techniques such as TEM/SEM.
- Use of only one dye (methylene blue) for photocatalytic evaluation.
- Laboratory conditions may differ from real wastewater systems.
- Limited optimization of key parameters such as pH, catalyst dosage, and oxidants.

## **1.4 Research Objectives**

### **General Objective**

The general objective of this study is to synthesize eco-friendly carbon quantum dots (CQDs) from mango peel waste using a hydrothermal method and evaluate their photocatalytic performance in degrading methylene blue under UV and sunlight irradiation.

### **Specific Objectives**

#### **Specific Objectives:**

- To synthesize CQDs from mango peel using a hydrothermal method and obtain a stable dispersion .
- To characterize CQDs using UV–Vis spectroscopy (200–800 nm) and observe fluorescence under UV light
- To analyze surface functional groups using FTIR spectroscopy.
- To evaluate the photocatalytic degradation of methylene blue using CQDs under UV and sunlight irradiation.
- To compare degradation efficiency under UV and sunlight based on absorbance changes over time.

## **1.5 Significance/Rationale of the Study**

This research holds significance from multiple perspectives, including environmental, scientific, economic, and socio-technical aspects. These dimensions collectively highlight the importance and relevance of the present study.

### **1.5.1 Environmental Significance**

Dye effluents from textile and allied industries contribute heavily to the pollution of water resources, with methylene blue emerging as one of the most prevalent pollutants among them [19]. In many developing countries such as Nepal, where treatment facilities for wastewater are scarce, dye-laden wastewater is commonly disposed of into rivers [13]. Globally, the textile industry is estimated to discharge approximately 200,000 tonnes of synthetic dyes into water bodies annually, representing one of the most significant sources of industrial wastewater contamination [24]. Synthetic dyes are broadly classified into several categories based on their chemical structure and application method, including azo dyes, anthraquinone dyes, triphenylmethane dyes, and heterocyclic dyes, among which azo dyes constitute nearly 70% of all commercially produced dyes worldwide [25]. Methylene blue (MB), a cationic thiazine dye belonging to the phenothiazine family, is extensively used in textile dyeing, paper printing, leather tanning, and biological staining owing to its strong tinctorial properties and chemical stability [26]. Its widespread industrial application, combined with its high aqueous solubility and resistance to conventional degradation, renders it a persistent and recalcitrant contaminant in receiving water bodies. Conventional wastewater treatment technologies including coagulation-flocculation, sedimentation, ion exchange, and membrane filtration have demonstrated limited efficacy in the complete removal of synthetic dyes, owing to the stability of dye molecules and the high operational costs associated with advanced treatment systems [27]. Biological treatment methods, while cost-effective under ideal conditions, are similarly constrained by the recalcitrance of synthetic dyes to microbial degradation and the sensitivity of activated sludge systems to fluctuating dye concentrations and pH conditions [28, 29]. These limitations have driven considerable research interest toward advanced oxidation processes (AOPs) and photocatalytic degradation as promising alternative strategies for the effective mineralization of dye pollutants in wastewater streams [30]. In this context, semiconductor-based and carbon nanomaterial-based photocatalysts, including carbon quantum dots, have attracted significant attention as cost-effective, environmentally benign, and highly efficient materials for the photodegradation of methylene blue and other persistent organic dye pollutants [31, 3].

### **1.5.2 Environmental Significance**

The present study demonstrates that carbon quantum dots (CQDs) synthesized from mango peel waste are capable of degrading methylene blue dye, indicating their potential application in wastewater treatment [32]. In addition to their functional performance, the utilization of mango peel as a precursor contributes to environmental sustainability by promoting proper waste management practices. Instead of being discarded in landfills, where organic waste contributes to greenhouse gas emissions, mango peel is converted into a value-added nanomaterial [21, 33]. This approach aligns with the principles of green chemistry and circular economy by transforming waste into

useful resources.

### **1.5.3 Scientific Significance**

From a scientific perspective, this study contributes to the expanding field of biomass-derived carbon quantum dots. The use of mango peel as a precursor for photocatalytic dye degradation offers a novel alternative to previously studied biomass sources such as papaya and mangosteen peels [17, 18].

The study further investigates the interaction of CQDs with different light sources, including ultraviolet irradiation and natural sunlight, providing insights into their practical applicability under real-world conditions. Characterization techniques such as UV–Visible spectroscopy and Fourier Transform Infrared (FTIR) analysis were employed to examine the optical properties and surface functional groups of the synthesized CQDs. These analyses help establish a relationship between the physicochemical properties of CQDs and their photocatalytic performance [23, 34].

Additionally, the results suggest that the degradation mechanism involves initial adsorption of the dye molecules onto the CQD surface, followed by photocatalytic breakdown under light irradiation. Another important contribution of this study lies in demonstrating that meaningful nanomaterial synthesis and analysis can be carried out using relatively simple laboratory setups. This highlights the feasibility of conducting advanced research in resource-limited environments [6].

### **1.5.4 Economic and Sociotechnical Significance**

The use of mango peel, a low-cost and abundantly available agricultural waste, makes this approach economically viable [35, 22]. The hydrothermal synthesis process employed in this study requires minimal and commonly available laboratory equipment, offering a cost-effective alternative to conventional photocatalysts [22].

Furthermore, the utilization of sunlight as a light source for photocatalytic degradation significantly reduces operational energy costs, enhancing the practicality of the method for small-scale and decentralized applications. The conversion of agricultural waste into functional nanomaterials also supports sustainable development practices and promotes resource efficiency [33].

### **1.5.5 Contribution to the Local Research Landscape**

Research on the green synthesis of nanomaterials from locally available agricultural waste remains limited in Nepal, where nanoscience is still an emerging field [21]. This study, conducted at Tribhuvan University using locally sourced mango peel, demonstrates that impactful nanomaterial research can be performed using existing laboratory facilities. It contributes to the development of local research capacity and encourages the exploration of indigenous resources for advanced scientific applications.

These results will serve as an important base for future research in many aspects like better synthesis techniques, composite materials, and wastewater purification.

## 2. Literature Review

### 2.1 Introduction to Carbon Quantum Dots

A family of zero-dimensional carbon-based nanomaterials known as carbon quantum dots (CQDs) has particles that are usually less than 10 nm. Since their accidental discovery in 2004 while single-walled carbon nanotubes were being purified [36], CQDs' unique physicochemical characteristics have garnered a lot of interest. These materials differ from traditional semiconductor quantum dots that include dangerous heavy metals like cadmium and lead because of their powerful and adjustable photoluminescence, high aqueous solubility, chemical stability, and low toxicity [2, 3].

The origin of photoluminescence in CQDs is complex and has been widely studied. Two principal mechanisms are commonly proposed: quantum confinement effects arising from the nanoscale carbon core and surface-state emissions associated with functional groups present on the particle surface [37]. In biomass-derived CQDs, the latter mechanism is particularly dominant due to the abundance of oxygen-containing groups such as hydroxyl ( $-\text{OH}$ ), carbonyl ( $\text{C}=\text{O}$ ), and carboxyl ( $-\text{COOH}$ ). These groups introduce localized energy states and defects, resulting in excitation-dependent emission behavior. This tunability of optical properties is one of the key features that make CQDs suitable for sensing and photocatalytic applications.

### 2.2 Synthesis of Carbon Quantum Dots

#### 2.2.1 Top-Down Approaches

Top-down approaches involve the breakdown of bulk carbon materials into nanoscale particles through physical or chemical means. Techniques such as arc discharge, laser ablation, electrochemical oxidation, and strong acid oxidation have been extensively used for CQD synthesis [34]. In these methods, large carbon structures are fragmented into smaller domains under high-energy conditions.

Arc discharge methods utilize high-temperature plasma generated between graphite electrodes, leading to the formation of carbon nanoparticles. Laser ablation involves the irradiation of carbon targets using high-energy laser pulses, which vaporize the material and subsequently condense into nanoscale particles. Electrochemical oxidation employs graphite electrodes in an electrolyte solution, where controlled oxidation leads to the formation of CQDs.

Despite their effectiveness, these methods are associated with several limitations. They typically require harsh reaction conditions, expensive equipment, and complex procedures. Moreover, the

resulting CQDs often possess limited surface functionalization, which restricts their interaction with target molecules in sensing and catalytic applications. These drawbacks have led to increased interest in alternative synthesis routes.

### **2.2.2 Bottom-Up Approaches**

Bottom-up approaches involve the synthesis of CQDs from molecular precursors through processes such as carbonization, polymerization, and nucleation. These methods are widely preferred for biomass-derived CQDs due to their simplicity, scalability, and compatibility with environmentally sustainable practices [38].

In bottom-up synthesis, small organic molecules or biomass-derived compounds undergo thermal or chemical transformation to form carbonaceous nanoparticles. The process typically involves dehydration of organic molecules, followed by condensation and polymerization reactions, leading to the formation of carbon nuclei. These nuclei subsequently grow into nanostructured CQDs.

An important advantage of bottom-up methods is the ability to control surface chemistry. Functional groups originating from the precursor are retained or formed during synthesis, enabling enhanced solubility, optical tunability, and chemical reactivity. This makes bottom-up methods particularly suitable for applications involving adsorption, sensing, and photocatalysis.

### **2.2.3 Hydrothermal Synthesis**

Hydrothermal synthesis is one of the most widely employed bottom-up techniques for CQD production, especially when using biomass precursors. In this method, an aqueous solution containing the precursor is sealed in a Teflon-lined autoclave and heated at multiplied temperatures, typically between 120 and 250°C.

The formation of CQDs during hydrothermal synthesis involves a sequence of thermochemical transformations. Initially, organic compounds present in the precursor undergo dehydration reactions, leading to the formation of intermediate species such as hydroxymethylfurfural and furfural. These intermediates then undergo condensation and polymerization, forming larger carbon-rich structures. As the reaction progresses, these structures undergo aromatization and nucleation, resulting in the formation of nanoscale carbon domains. Continued carbonization leads to the development of CQDs with functionalized surfaces.

A key characteristic of hydrothermal synthesis is the preservation of oxygen-containing functional groups on the CQD surface. These groups enhance the hydrophilicity and stability of CQDs in aqueous media and play a crucial role in determining their optical and catalytic properties. Reaction parameters such as temperature, time, and precursor concentration significantly influence the size, crystallinity, and surface chemistry of the resulting CQDs. Lower temperatures tend to preserve functional groups, while higher temperatures promote greater carbonization and structural

ordering.

Expanding beyond pyrolysis-based routes, hydrothermal synthesis has emerged as a more controllable and environmentally benign strategy for producing mango peel-derived CQDs. Malitha et al. explored direct hydrothermal treatment of dried mango peel powder at 200°C for 10 h, demonstrating the feasibility of water as the sole solvent for carbonization, though the fluorescence quantum yield remained modest at 0.6%. In a more recent systematic study, CQDs were synthesized from mango peels via green hydrothermal treatment at 200°C for varying durations (3–15 h), revealing that synthesis time significantly influences optical behavior, with photoluminescence emission wavelengths ranging from 441 to 447 nm and optical bandgap values between 3.825 and 3.935 eV. The CQDs synthesized at 3 h exhibited the smallest average particle size of 3.54 nm with a high carbon content of 97%, and were monodispersed as confirmed by TEM [35]

## 2.2.4 Pyrolysis

Pyrolysis involves the thermal decomposition of organic precursors at high temperatures, typically above 200°C, in the absence of oxygen. This method facilitates rapid carbonization and the formation of graphitic carbon structures. Compared to hydrothermal synthesis, pyrolysis often produces CQDs with a more developed carbon core and higher degree of graphitization.

However, the high-temperature conditions associated with pyrolysis can lead to the removal of oxygen-containing functional groups, resulting in reduced surface functionality. This can limit the interaction of CQDs with pollutants and metal ions, which is essential for applications such as sensing and photocatalysis. Nevertheless, pyrolysis-derived CQDs often exhibit strong photoluminescence due to the presence of well-defined  $sp^2$  carbon domains. The choice of organic precursor plays a pivotal role in determining the structural and optical characteristics of the resulting CQDs. A diverse range of precursors has been reported, including citric acid [39], glucose [38], sucrose [40] and natural biomass sources such as grass, fruit peels, and chitosan [41]. The molecular composition of the precursor governs the heteroatom content, surface functional group density, and quantum yield of the synthesized CQDs. Nitrogen-rich precursors, for instance, have been widely employed to introduce nitrogen dopants into the carbon framework, which significantly enhances photoluminescence quantum yields by creating additional emissive surface states [42].

## 2.2.5 Microwave-Assisted Synthesis

Microwave-assisted synthesis has emerged as a rapid and energy-efficient alternative to conventional methods. In this approach, microwave radiation is used to heat the precursor solution, enabling uniform and volumetric heating. This results in significantly reduced reaction times, often on the order of minutes compared to several hours required for hydrothermal synthesis.

The rapid heating mechanism promotes efficient carbonization and nucleation, leading to the

formation of CQDs with comparable optical properties. However, precise control over reaction conditions can be challenging, particularly when using complex biomass precursors. This may result in variations in particle size distribution and surface functionalization. The mechanistic basis of microwave-assisted synthesis distinguishes it fundamentally from conventional thermal heating methods. In conventional heating, energy is transferred from the external heat source to the reaction vessel and subsequently to the solvent and solute through conduction and convection, resulting in thermal gradients and non-uniform temperature distribution. Microwave irradiation, by contrast, couples directly with polar molecules and ionic species in the reaction mixture through dipolar polarization and ionic conduction mechanisms, generating heat volumetrically and instantaneously throughout the entire solution [43]. This dielectric heating mechanism ensures highly uniform thermal treatment of the precursor material, which is a critical determinant of the monodispersity and optical uniformity of the resulting CQDs. The frequency of microwave radiation employed in laboratory synthesis, typically 2.45 GHz, corresponds to a photon energy insufficient to induce direct chemical bond cleavage, thereby confirming that the observed accelerated reaction kinetics arise solely from the thermal effects of rapid and homogeneous heating rather than any non-thermal microwave effect [44]. The superheating of solvents above their conventional boiling points, achievable under closed-vessel microwave conditions, further accelerates the carbonization and dehydration reactions that are integral to CQD formation [45].

Despite these limitations, microwave-assisted synthesis is considered a promising technique due to its energy efficiency and potential for rapid production of CQDs. It is particularly suitable for applications where synthesis speed is a critical factor. Beyond the synthesis of conventional CQDs, microwave-assisted methods have been adapted for the fabrication of surface-passivated and functionalized CQDs in a single step. The simultaneous carbonization and surface modification achievable under microwave conditions represent a significant processing advantage over post-synthetic functionalization strategies required by other methods [42, 3]. This one-pot capability makes microwave synthesis particularly attractive for the preparation of CQDs tailored for specific applications in biosensing, photocatalysis, and heavy metal ion detection, where precise surface chemistry is paramount [6, 3].

### **2.2.6 Biomass-Derived CQDs**

The use of biomass as a precursor has gained significant attention due to its sustainability, low cost, and abundance. Agricultural waste materials such as fruit peels, rice husk, and plant extracts have been successfully used to produce CQDs [46].

Fruit peels are particularly advantageous due to their high content of carbohydrates, phenolic compounds, and natural heteroatoms. These components facilitate efficient carbonization and functionalization.

Mango peel (*Mangifera indica*) is a promising precursor due to its rich composition of polyphenols, flavonoids, cellulose, and pectin. Jiao et al. synthesized CQDs from mango peel via pyrolysis and demonstrated their photoluminescent properties and metal ion sensing capability [47]. Singh et al. further reported blue-emitting CQDs with emission peaks around 430–450 nm using a one-pot pyrolysis method [48]. However, hydrothermal synthesis of mango peel-derived CQDs remains relatively less explored, particularly for photocatalytic applications. In the context of photocatalytic applications, mango peel-derived CQDs have been explored as co-catalysts in nanocomposite systems. Carbon quantum dots synthesized from mango waste peels via a facile hydrothermal process were coated onto cobalt-zinc ferrite (CZF) nanoparticles through an in-situ oxidative method to fabricate a CZF@CQDs nanophotocatalyst. The resulting nanocomposite exhibited a narrow band gap of 1.20 eV suitable for visible light absorption, and demonstrated approximately 95% degradation efficiency for Reactive Blue 222 and Reactive Yellow 145 dyes within 25 minutes under visible light irradiation, with recyclability maintained at approximately 82% efficiency even after seven cycles [49].

Beyond mango peel, other fruit peel-derived CQDs have similarly demonstrated photocatalytic potential. CQDs prepared by one-step hydrothermal treatment of avocado peel waste using only water as solvent were evaluated for the photocatalytic removal of methyl orange (MO) dye, achieving a removal efficiency of approximately 78%, with performance directly dependent on solution pH and nanomaterial dosage. [50]. Likewise, green fluorescent CQDs synthesized hydrothermally from pear juice exhibited excellent visible-light-induced photocatalytic activity, achieving 99.5% degradation of methylene blue within 130 minutes, while also functioning as dual-mode fluorescent nanoprobes for the selective detection of Fe(III) and ascorbic acid through photoluminescence turn-off and turn-on mechanisms[51].

## 2.3 Characterization of Carbon Quantum Dots

The characterization of carbon quantum dots (CQDs) is essential for understanding their structural, optical, and chemical properties, which directly influence their performance in sensing and photocatalytic applications. A combination of spectroscopic and analytical techniques is typically employed to obtain a comprehensive understanding of CQD behavior.

UV–Visible (UV–Vis) spectroscopy is one of the primary techniques used to investigate the optical properties of CQDs. The absorption spectrum provides information about electronic transitions within the carbon structure. Typically, CQDs exhibit a strong absorption band in the ultraviolet region, which is associated with  $\pi-\pi^*$  transitions of aromatic C=C bonds present in  $sp^2$  hybridized carbon domains. This transition generally appears in the wavelength range of 260–280 nm. In addition, a secondary absorption feature or shoulder is often observed between 280 and 330 nm, which is attributed to  $n-\pi^*$  transitions arising from non-bonding electrons of oxygen-containing

functional groups such as carbonyl (C=O) moieties [52].

The relative intensity and position of these absorption peaks provide valuable insights into the degree of carbonization, surface oxidation, and conjugation within the CQDs. For instance, a pronounced  $n-\pi^*$  transition indicates a higher density of surface functional groups, which is particularly important for applications involving adsorption and chemical interactions.

Photoluminescence (PL) spectroscopy is another critical technique used to evaluate the emission characteristics of CQDs. Biomass-derived CQDs typically exhibit strong blue or blue-green emission under ultraviolet excitation. One of the defining features of CQDs is their excitation-dependent emission behavior, in which the emission wavelength shifts with changes in excitation wavelength. This phenomenon is attributed to the presence of multiple emissive sites, arising from variations in particle size, surface states, and functional group distribution [37].

The origin of photoluminescence in CQDs is generally explained by a combination of quantum confinement effects and surface-state emissions. In smaller particles, quantum confinement leads to discrete energy levels, resulting in size-dependent emission. However, in biomass-derived CQDs, surface defects and functional groups play a more dominant role, creating localized energy states that contribute to emission. These surface states are particularly sensitive to environmental conditions, making CQDs highly responsive in sensing applications.

Fourier Transform Infrared (FTIR) spectroscopy is employed to identify the functional groups present on the surface of CQDs. The FTIR spectrum of CQDs typically exhibits a broad absorption band in the range of 3200–3500  $\text{cm}^{-1}$ , corresponding to O–H stretching vibrations. Peaks near 1700  $\text{cm}^{-1}$  are attributed to C=O stretching, indicating the presence of carbonyl or carboxyl groups. Additionally, bands in the range of 1000–1250  $\text{cm}^{-1}$  correspond to C–O stretching vibrations, confirming the presence of alcohols, ethers, or esters [2]. The technique operates on the basis of molecular vibrations, including stretching and bending modes. When infrared radiation is incident upon a sample, molecules selectively absorb photons whose energy matches the energy difference between vibrational energy levels. This absorption is only IR-active when the vibration results in a net change in the dipole moment of the molecule, as governed by the selection rules of quantum mechanics [53].

These functional groups are of critical importance, as they determine the hydrophilicity, colloidal stability, and chemical reactivity of CQDs. Furthermore, they act as active sites for interaction with metal ions and organic pollutants, thereby enhancing adsorption and catalytic efficiency. The surface oxygen-containing functional groups identified through FTIR analysis are of particular significance for CQDs, as they directly influence the photoluminescence behavior, colloidal stability, and biocompatibility of these nanomaterials [37]. FTIR spectroscopy thus serves as an indispensable tool in the systematic characterization of CQDs, providing complementary information alongside other techniques such as X-ray photoelectron spectroscopy (XPS) and Raman

spectroscopy.

In addition to these techniques, advanced characterization methods such as transmission electron microscopy (TEM), scanning electron microscopy (SEM), and X-ray diffraction (XRD) are often used to analyze particle size, morphology, and crystallinity. TEM images typically reveal quasi-spherical particles with sizes below 10 nm, while XRD patterns indicate amorphous or partially graphitic structures. Together, these techniques provide a comprehensive understanding of CQD structure and behavior.

## **2.4 Applications in Environmental Remediation and Sensing**

### **2.4.1 Metal Ion Sensing**

Carbon quantum dots have been extensively investigated for the detection of metal ions due to their strong photoluminescence and surface reactivity. Among various metal ions,  $\text{Fe}^{3+}$  has received particular attention because of its environmental and biological significance.

The sensing mechanism of CQDs is generally based on fluorescence quenching, which occurs when  $\text{Fe}^{3+}$  ions interact with the surface functional groups of CQDs. This interaction can take place through coordination bonding between  $\text{Fe}^{3+}$  ions and oxygen-containing groups such as  $-\text{COOH}$  and  $\text{C}=\text{O}$ . The formation of such complexes facilitates electron or energy transfer processes, leading to a reduction in fluorescence intensity [47].

Two primary quenching mechanisms are typically involved: static quenching and dynamic quenching. Static quenching occurs when a non-fluorescent complex is formed between CQDs and metal ions, while dynamic quenching involves collisional interactions between excited CQDs and metal ions. In many cases, both mechanisms may operate simultaneously.

In addition to fluorescence-based sensing, CQDs can also be used for UV–Visible absorbance-based detection. In this approach, the presence of metal ions leads to measurable changes in the absorbance spectrum of CQDs, often due to aggregation effects or alterations in electronic structure. Although less commonly reported, absorbance-based sensing offers advantages in terms of simplicity and cost-effectiveness, as it does not require specialized fluorescence instrumentation.

### **2.4.2 Photocatalytic Degradation**

The photocatalytic activity of CQDs has attracted significant interest for environmental remediation, particularly in the degradation of organic pollutants such as dyes. CQDs act as light-absorbing materials that can generate electron-hole pairs upon irradiation.

When CQDs are exposed to light, photons with sufficient energy excite electrons from the valence band to the conduction band, leaving behind holes in the valence band. These charge carriers can then participate in redox reactions. The excited electrons react with dissolved oxygen to produce superoxide radicals ( $\text{O}_2^{\bullet-}$ ), while the holes oxidize water or hydroxide ions to generate

hydroxyl radicals ( $\bullet\text{OH}$ ). These reactive oxygen species (ROS) are highly oxidative and can degrade organic pollutants into smaller, less harmful molecules, eventually leading to complete mineralization.

The efficiency of photocatalysis depends on several factors, including light absorption capability, charge separation efficiency, and surface interaction with pollutants. The presence of surface functional groups enhances adsorption of dye molecules onto the CQD surface, increasing the proximity between reactive sites and pollutants. This improves the overall degradation rate.

Studies using biomass-derived CQDs, particularly from fruit peels, have demonstrated effective photocatalytic degradation of methylene blue [54]. The enhanced performance is often attributed to improved charge transfer and reduced recombination of electron-hole pairs.

### **2.4.3 UV vs Sunlight Photocatalysis**

Most photocatalytic studies involving CQDs are conducted under ultraviolet (UV) irradiation due to its high photon energy, which facilitates efficient electron excitation. However, the practical application of UV-based systems is limited by high energy requirements and the low proportion of UV radiation in natural sunlight, which constitutes less than 5% of the solar spectrum.

In contrast, sunlight-driven photocatalysis offers a more sustainable and cost-effective alternative. CQDs possess the ability to absorb both UV and visible light, making them suitable for solar-driven applications. Their broad absorption spectrum and unique electronic structure allow them to utilize a larger portion of the solar spectrum compared to traditional photocatalysts such as  $\text{TiO}_2$ .

Despite these advantages, comparative studies evaluating the performance of CQDs under UV and natural sunlight conditions remain limited. Such comparisons are essential for assessing the practical applicability of CQDs in real-world environmental systems. In general, photocatalytic reactions under UV light tend to be faster due to higher photon energy, whereas sunlight-driven processes offer better sustainability and scalability.

Understanding the differences in performance under these two conditions is critical for optimizing CQD-based systems for environmental remediation. This aspect forms an important component of the present study, where the photocatalytic degradation of methylene blue is evaluated under both UV irradiation and natural sunlight.

## **2.5 Research Gap and Justification**

### **2.5.1 Research Gap**

Despite extensive research on carbon quantum dots (CQDs), several important gaps remain, particularly in the context of biomass-derived CQDs for environmental applications:

**1. Limited focus on photocatalysis:**

Mango peel-derived CQDs have predominantly been studied for sensing and bioimaging applications, with very limited research on their use in photocatalytic dye degradation (Jiao et al., 2019; Singh et al., 2020).

**2. Underexplored hydrothermal synthesis route:**

Most existing studies employ pyrolysis methods, while hydrothermal synthesis—known for preserving oxygen-containing functional groups essential for photocatalysis—remains insufficiently explored.

**3. Lack of systematic photocatalytic evaluation:**

There is a lack of comprehensive studies investigating the photocatalytic performance of mango peel-derived CQDs, particularly for organic dye degradation.

**4. Absence of comparative irradiation studies:**

Comparative analysis under ultraviolet (UV) and natural sunlight conditions is rarely reported, limiting understanding of real-world applicability.

**5. Limited use of UV–Vis absorbance-based analysis:**

Most studies rely on photoluminescence techniques, with minimal emphasis on UV–Vis absorbance spectroscopy for evaluating photocatalytic efficiency.

## **2.5.2 Justification of the Study**

This study is designed to address the above research gaps through the following contributions:

- It develops a low-cost and eco-friendly approach for wastewater treatment using waste biomass (mango peel).
- It utilizes sustainable and locally available resources, enhancing environmental and economic feasibility.
- It applies hydrothermal synthesis, enabling better surface functionalization for improved photocatalytic activity.
- It evaluates practical applicability by comparing performance under UV and natural sunlight conditions.
- It provides an alternative to conventional costly wastewater treatment methods, supporting sustainable environmental remediation.

## 3. Methodology

### 3.1 Materials

#### 3.1.1 Source of Raw Material

Fresh mango (*Mangifera indica*) peels were selected as the carbon precursor for CQD synthesis in this study owing to their high carbon content, abundant surface functional groups, low cost, and ready availability as an agro-industrial waste product[47, 55]. The peels were collected from a local fruit market in Kathmandu, Nepal. Only ripe, disease-free mangoes were chosen to maintain batch-to-batch consistency in the organic composition of the precursor material.

#### 3.1.2 Chemicals and Reagent

Methylene blue (MB; molecular formula  $C_{16}H_{18}ClN_3S$ , molecular weight =  $319.85 \text{ g mol}^{-1}$ , purity  $\geq 99\%$ ) was used as the model organic pollutant in all photocatalytic degradation experiments. It was chosen due to the following reasons: It is a cationic dye extensively employed within the textile and paper industry; it possesses a distinct absorption peak at  $\lambda_{\text{max}} = 664 \text{ nm}$ ; its aqueous concentration can be precisely measured via UV–Visible spectroscopy[56]. All rinsing processes, solutions, and dilutions used in the experiment utilized distilled water. Ethanol of analytical grade was used for the cleaning of grinding apparatuses to avoid any organic contamination of the precursor material. For the synthesis of CQDs, no other chemicals were needed except for the ones found in the biomass of the mango peel[38].

### 3.2 Synthesis of Carbon Quantum Dots from Mango Peel

#### 3.2.1 Raw Material Preparation

In order to reduce microbiological deterioration and compositional change, the mango peels that were gathered from the market were processed right away. The following stages were taken in order during the preparation process:

- **Washing:** The collected mango peels were first rinsed thoroughly under running tap water for approximately 5 minutes to remove surface impurities such as dirt and dust. Subsequently, the peels were washed three times with distilled water to eliminate any remaining contaminants.
- **Cutting:** The cleaned peels were cut into smaller pieces (approximately  $1\text{--}2 \text{ cm}^2$ ) using a clean stainless-steel knife. This step ensured uniform drying and improved efficiency during

the grinding process.

- **Drying:** The cut peels were dried in a forced hot air oven at 50°C for 8 hours. The temperature was carefully selected to effectively remove moisture while preventing thermal degradation of the natural organic components present in the peel. Drying was considered complete when a constant weight (gravimetric stability) was achieved.
- **Grinding:** The dried peel pieces were ground into a fine powder using an electric laboratory grinder. Prior to use, the grinder was thoroughly cleaned with tap water, followed by distilled water, and finally rinsed with analytical-grade ethanol to avoid contamination.
- **Storage:** The obtained mango peel powder (MPP) was stored in a clean, airtight glass container and kept in a cool, dry environment. This prevented moisture absorption from the surroundings and ensured consistency in the precursor-to-water ratio during subsequent synthesis.

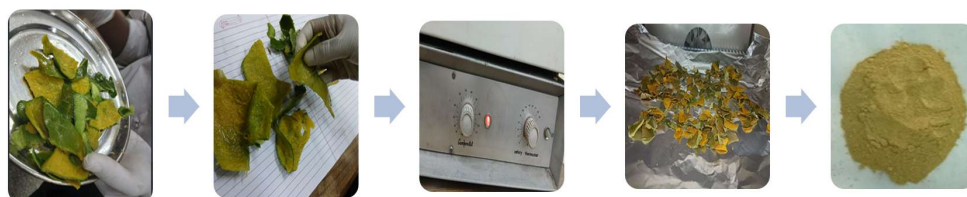


Figure 3.1: Diagrammatic representation of the preparation of raw material

### 3.2.2 Hydrothermal Synthesis of CQDs

Carbon quantum dots (CQDs) were synthesized by adopting an easy single-step hydrothermal process, wherein the organic components of biomass are transformed to carbon nanoparticles through hydrothermal treatment without the requirement of any other chemicals.[38]. About 5.0 g of mango peel powder was weighed using an analytical balance and placed in a 250 mL beaker, and then 100 mL of distilled water was used to make the initial mixture.

### 3.2.3 Preparation of the Precursor Suspension

The mixture was stirred continuously using a magnetic stirrer at room temperature (around 25°C) for 30 minutes. This step ensured a uniform suspension and allowed water-soluble components such as sugars, polyphenols, and organic acids to dissolve. These compounds act as the main carbon source and contribute to the surface functional groups of the CQDs during the hydrothermal process[47, 37]

### 3.2.4 Hydrothermal Carbonisation

Following stirring, the prepared suspension was carefully transferred into a 200 mL Teflon-lined stainless steel autoclave. The autoclave was sealed tightly to maintain autogenous pressure during the reaction. The sealed autoclave was placed in a muffle furnace and heated to 130°C, where it was maintained for 12 hours[38]. After the 12-hour reaction, the furnace was switched off and the autoclave was allowed to cool naturally inside the furnace for approximately 4–5 hours until it reached room temperature. Rapid cooling was avoided to prevent thermal shock to the Teflon liner. Upon opening, a brownish-yellow coloured liquid product was observed, indicative of CQD formation[38].



Figure 3.2: Diagrammatic representation of the Hydrothermal process

## 3.3 Photocatalytic Degradation of Methylene Blue using Mango Peel CQDs

### 3.3.1 Methylene Blue Solution Preparation

- A 10 mg/L methylene blue (MB) solution ( $\lambda_{\max} \approx 664$  nm) was prepared.
- 50 mL of MB solution was used for each experiment.
- Initial absorbance was recorded at 664 nm using a UV–Vis spectrophotometer.

### 3.3.2 Adsorption–Desorption Equilibrium Study

- 5 mL of CQD solution was added to the MB solution.
- The mixture was stirred and kept in the dark for 30 minutes to achieve equilibrium.

### 3.3.3 Photocatalytic Reaction

The reaction mixture was exposed to light (UV and sunlight) with continuous stirring.

### 3.3.4 Sampling and Analysis

- Aliquots were withdrawn at 0, 15, 30, 60, and 90 minutes.
- Samples were centrifuged at 8000 rpm for 10 minutes.
- Absorbance of the supernatant was measured at 664 nm.

### 3.3.5 Degradation Efficiency Calculation

Degradation efficiency (%) was calculated using:

$$\text{Degradation Efficiency (\%)} = \frac{A_0 - A_t}{A_0} \times 100 \quad (3.1)$$

## 3.4 Purification of the CQD Suspension

The product obtained after hydrothermal synthesis contained CQDs along with unreacted residues and larger particles. Therefore, a simple purification process was carried out to obtain a clear and stable CQD solution:

- **Settling:** The solution was transferred to a clean vial and left undisturbed for about 2 hours to allow heavier particles to settle at the bottom.
- **Decantation:** The clear upper layer containing CQDs was carefully collected without disturbing the settled particles.
- **Dilution:** The collected solution was diluted with distilled water in a 1:1 ratio to obtain a stable working solution suitable for analysis [2, 3].

## 3.5 Characterisation of the Synthesised CQDs

Various spectroscopic techniques are used to analyse the optical properties and surface chemistry of the synthesized CQDs.

### 3.5.1 UV-Visible Absorption Spectroscopy

Optical absorption characteristics of the purified CQD sample were determined by UV-Vis spectrophotometry from a wavelength range of 200 to 800 nm. The reference standard used for the experiment was distilled water and quartz cuvettes with a 1-cm path length were used throughout the analysis..

To find distinctive electronic transitions, the absorbance spectra was recorded. The aromatic C=C bonds'  $\pi \rightarrow \pi^*$  transition is responsible for the peak seen in the lower wavelength area, whilst

the  $n \rightarrow \pi^*$  transition linked to surface carbonyl (C=O) groups is responsible for the shoulder or peak at higher wavelengths. These transitions are usually seen in the 250–320 nm range for CQDs produced from biomass [17, 57].

### 3.5.2 Photoluminescence (Fluorescence) Analysis

The fluorescence behaviour of the synthesised CQDs was evaluated both qualitatively and quantitatively.

**Visual fluorescence observation:** CQD solutions were prepared in different solvent systems (undiluted, ethanol-diluted 1:1, and water-diluted 1:1) and exposed to UV light at 254 nm and 365 nm using a UV chamber[47]

**Comparative solvent effect study:** The CQD solutions (undiluted, ethanol-diluted, and water-diluted) were compared under UV light to observe changes in fluorescence. This helped to understand how different solvents influence the emission behavior of CQDs.

### 3.5.3 Fourier Transform Infrared (FTIR) Spectroscopy

The emitted fluorescence colour and intensity were observed. Green emission under 254 nm and blue emission under 365 nm indicated successful CQD formation and the presence of different surface emissive states.

FTIR analysis: The surface functional groups of the produced CQDs were identified using Fourier Transform Infrared (FTIR) spectroscopy (PerkinElmer Spectrum IR, Version 10.6.2, ASCOL Campus). The spectra were captured between 4000 and 500  $\text{cm}^{-1}$ .

The main absorption peaks observed are typically assigned as follows:

- Broad O–H stretching around 3200–3500  $\text{cm}^{-1}$  [37]
- C–H stretching at 2850–2960  $\text{cm}^{-1}$ [37]
- C=O stretching (carbonyl/carboxyl groups) at 1700–1740  $\text{cm}^{-1}$  [58]
- C=C stretching of aromatic structures at 1580–1620  $\text{cm}^{-1}$  [37]
- C–O stretching at  $\sim$ 1000–1250  $\text{cm}^{-1}$

The presence of these functional groups confirms the successful incorporation of oxygen-rich moieties on the CQD surface, which are essential for their colloidal stability and photocatalytic activity [37, 54]

## 3.6 Photocatalytic Degradation of Methylene Blue

### 3.6.1 Preparation of Methylene Blue Solution

A precisely weighed mass of methylene blue (MB) powder was dissolved in distilled water in a 1000 mL volumetric flask to create a stock solution of MB at a concentration of  $10 \text{ mg} \cdot \text{L}^{-1}$ . The solution was stored in an amber glass bottle to prevent photodegradation prior to use. The absorption maximum of this stock solution was confirmed at  $\lambda_{\text{max}} = 664 \text{ nm}$  using a UV-Vis spectrophotometer, with an initial absorbance of  $A_0 = 1.315$  (using a 1 cm path length cuvette)[54, 37].

### 3.6.2 Dark Adsorption Equilibration

For each photocatalytic experiment, 50 mL of the  $10 \text{ mg} \cdot \text{L}^{-1}$  MB stock solution was transferred into a 100 mL glass beaker. An appropriate volume of the CQD stock solution was added, and the mixture was magnetically stirred in complete darkness for 30 minutes prior to light irradiation. This dark equilibration period is essential to establish an adsorption-desorption equilibrium between MB molecules and the CQD catalyst surface, thereby decoupling the contribution of surface adsorption from true photocatalytic degradation [54, 22]. Any decrease in MB absorbance during this dark period is attributed solely to adsorption, not photodegradation.

### 3.6.3 Light Irradiation Setup

After dark equilibration, the samples were irradiated by two sources of radiation in order to investigate the efficiency of the photocatalysis process both in the lab and under natural conditions:

- **Artificial ultraviolet radiation:** In this case, the sample was exposed to the UV lamp which was set to shine on the reaction flask from a certain distance. The experiments were done in total darkness [49].
- **Natural sunlight:** The reaction beaker was placed outdoors on a clear sunny day (10:00 AM–2:00 PM) for obtaining peak solar intensity [22].

### 3.6.4 Sample Collection and Analysis

An aliquot of 2–3 mL was withdrawn from the mixture after every 15-minute interval (at 0 minutes - end of dark equilibration period, 15 minutes, 30 minutes, 60 minutes, and 90 minutes). All the withdrawn samples were centrifuged at 8000 rpm for 10 minutes in order to separate all the suspended CQD and MB aggregates, and the MB absorbance was determined only in solution. The absorbance at 664 nm was recorded using UV-Visible spectroscopy [54]. The measurement was performed promptly after centrifugation to minimise any further photodegradation during sample handling.

### 3.7 Degradation Efficiency Calculation

The photocatalytic degradation efficiency ( $\eta$ ) at each irradiation time point was calculated using the following expression:

$$\eta(\%) = \frac{A_0 - A_t}{A_0} \times 100 \quad (3.2)$$

where  $A_0$  is the initial absorbance of the MB solution at 664 nm measured at the end of the dark equilibration period (before light exposure), and  $A_t$  is the absorbance measured at irradiation time  $t$ . This equation is based on the assumption that the absorbance at 664 nm is directly proportional to the MB concentration according to the Beer–Lambert law, which was verified to be valid over the concentration range studied (0–10 mg L<sup>-1</sup>) [54]. A decrease in absorbance thus directly corresponds to a decrease in MB concentration caused by photocatalytic degradation.

### 3.8 Data Analysis and Graphical Representation

All absorbance values recorded at the five irradiation time points (0, 15, 30, 60, and 90 min) for both UV light and sunlight experiments were tabulated. Degradation efficiencies were calculated using the expression above for each time point. The following plots were generated to interpret the photocatalytic behaviour of the synthesised CQDs:

- **Absorbance vs. irradiation time:** Plots of  $A_t$  (at 664 nm) against time for both UV and sunlight exposure, showing the progressive bleaching of the MB solution.
- **Degradation efficiency vs. irradiation time:** Plots of  $\eta(\%)$  against time, used to compare the rates of photocatalytic degradation under UV and natural sunlight.
- **Comparative performance under UV light and sunlight:** Side-by-side comparison of the two irradiation sources to assess the potential of the CQDs for solar-driven water treatment applications [22].

All graphs were generated using *OriginPro* software (OriginLab Corporation, Northampton, MA, USA). Each experiment was conducted in triplicate, and the mean values with standard deviations are reported.

## 4. Results & Discussion

The peel waste from mango was sourced from a local market located in Nepal and used as a source material for the production of carbon quantum dots (CQDs). The source material was washed with distilled water in order to eliminate dirt and other contaminants, and dried under heat conditions of around 50 °C for 8-10 hours. The dried source material was then pulverized using a clean grinding machine.

In terms of synthesis methodology, an amount of mango peel powder was introduced in distilled water and stirred using a magnetic stirrer for around 30 minutes. The resultant mixture was added in a Teflon-lined stainless steel autoclave, which was heated up to 130 °C for around 12 hours. Post-completion of the reaction, the autoclave was cooled down to room temperature in the oven itself. The mixture was then filtered to obtain a clear solution of CQDs.

### 4.1 Hydrothermal Synthesis Mechanism

Hydrothermal processing is a common technique for the preparation of carbon-based nanomaterials owing to the simplicity, environmental benignity, and controllability of size and surface chemistry. Hydrothermal processing entails the reaction of organic feedstocks in an aqueous medium characterized by high temperatures and pressures in a closed system. During the process, the biomass is hydrolyzed, dehydrated, carbonized, and passivated to yield carbon nanostructures.

The overall process can be represented by the generalized reaction:



Hydrothermal synthesis is one of the most common methods that are employed in the preparation of carbon quantum dots. In hydrothermal synthesis, the complicated biological compounds like cellulose, hemicellulose, and lignin found in the mango peel undergo decomposition and rearrangement into carbon nuclei. The carbon nuclei develop further into carbon quantum dots possessing different oxygen functional groups, including hydroxyl, carbonyl, and carboxyl groups.

There are various parameters that affect the performance and features of the produced CQDs, such as the nature and amount of the precursors, the temperature and pressure conditions of the reaction, the time period required for the reaction to occur, and the pH level of the solution used. High temperatures contribute to the quick carbonization process and production of smaller nanoparticles, whereas reaction time determines the level of functionalization.

Therefore, careful optimization of these synthesis parameters is necessary to obtain CQDs with

desirable physicochemical properties suitable for photocatalytic applications.

## 4.2 Photocatalytic Degradation Mechanism of Methylene Blue (MB)

### Step 1: Light Absorption by CQDs

When CQDs are exposed to UV light or sunlight, they absorb light energy and become excited.



Electrons move to the conduction band, leaving holes in the valence band.

### Step 2: Formation of Reactive Species

The excited electrons react with oxygen to form superoxide radicals.

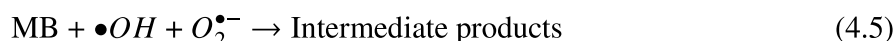


The holes react with water to form hydroxyl radicals.



### Step 3: Degradation of Methylene Blue

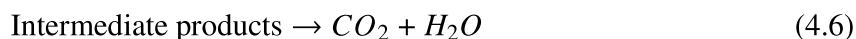
The reactive radicals attack the methylene blue dye molecules and break them into smaller compounds.



As the dye degrades, the absorbance at 664 nm decreases.

### Step 4: Mineralization

The intermediate compounds finally convert into harmless products.



## 4.3 Visual Appearance and Fluorescence Properties

When exposed to ambient light, the prepared CQDs resulted in a light yellow to dark brown colloidal suspension due to the carbonization of the mango peel biomass at 130°C. The color change is attributed to the presence of carbon-core nanoparticles that contain organic groups on their surface.[59]. Strikingly different optical behavior was observed under UV excitation. Under the UV curing chamber at 254 nm (short-wave UV), the solution emitted bright green fluorescence,

while at 365 nm (long-wave UV), bright blue fluorescence was observed. This dual-emission behavior is characteristic of quantum confinement effects and surface state emission in CQDs, and confirms the successful formation of photoluminescent nanoparticles[59]. The dependence of emission color on excitation wavelength is well documented for CQDs Duong et al. (2025) similarly reported blue-green photoluminescence with emission peaks red-shifting progressively at longer excitation wavelengths for hydrothermally synthesized CQDs[52].



Figure 4.1: Testing of the sample in the UV chamber

When examined under a UVA 365 nm lamp, the undiluted CQD solution showed fluorescence but with reduced clarity, attributed to concentration quenching and the presence of residual organic impurities.



Figure 4.2: Testing of Undiluted sample in the UVA 365nm lamp

Upon dilution with ethanol, bright bluish-green fluorescence was observed, and a comparable bluish-green emission appeared when the solution was diluted with distilled water. These observations across different solvent systems confirm the presence of well-dispersed CQDs with stable and favorable optical properties, as well as the influence of particle concentration and solvent polarity on emission intensity.

#### 4.4 UV-Vis Spectroscopic Characterization

Now, the produced CQDs' UV-Vis absorption spectra showed distinctive absorption characteristics in each of the three sample preparations:

- Normal (undiluted) sample: In normal sample we obtained the absorption at 200–280 nm with a shoulder near 270–290 nm, attributed to  $\pi-\pi^*$  transitions of the aromatic C=C core



Figure 4.3: Testing of Ethanol diluted sample in the UVA 365nm lamp

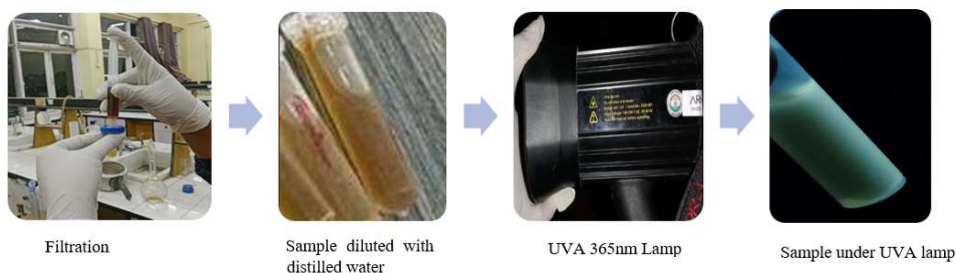
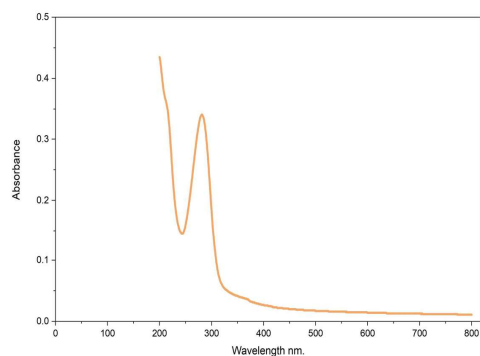


Figure 4.4: Testing of Distilled water diluted sample in the UVA 365nm lamp

and  $n-\pi^*$  transitions of C=O surface groups. The relatively low visible-range absorbance indicates smaller nanoparticle sizes and good dispersion.



Peak Wavelength	Max Absorbance	UV Range (280nm)
200-280 nm	0.435	0.339

Figure 4.5: Normal (Undiluted Sample)

- Ethanol diluted sample: In ethanol diluted sample we observed a sharp, prominent peak near 220–240 nm (C=C) and a distinct peak at 260–280 nm (C=O) is obtained. The sharper peaks suggest better CQD dispersion and reduced agglomeration in ethanol.

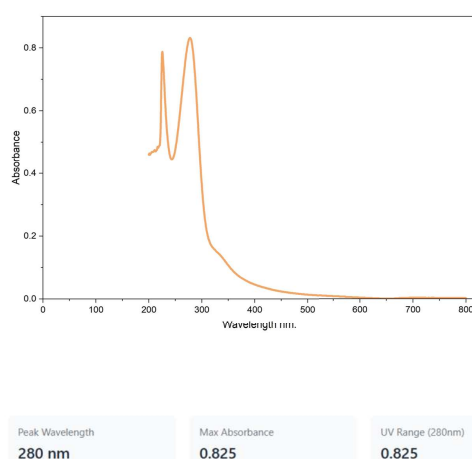


Figure 4.6: Ethanol Diluted Sample

water-diluted sample: FTIR results confirm the findings of studies carried out on other types of biomass. A diluted sample of the biomass in distilled water yielded the highest absorbance values, with a maximum at around 200–220 nm and a shoulder from 270–290 nm. The high absorbance value can be attributed to more oxygen-functional groups (-OH, -COOH) at the surface.

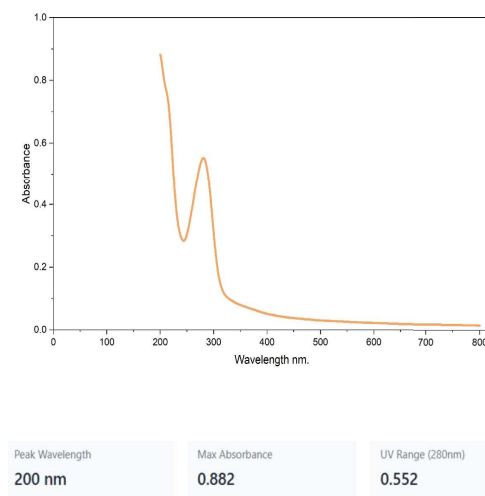


Figure 4.7: Distilled Water Sample

## 4.5 FTIR Characterization

For the purpose of determining the surface functional groups on CQDs prepared, FTIR Spectroscopy was used. The presence of some unique peaks in the FTIR Spectrum revealed information regarding the chemical environment around the surface of the CQDs.

FTIR Spectroscopy was used for the identification of the surface. A broad absorption band with the center at  $3334\text{ cm}^{-1}$  was assigned to O–H stretching vibrations, thus the surface hydroxyl groups and adsorbed water on the surface of the sample. A peak at  $2974\text{ cm}^{-1}$  was associated with C–H stretching vibrations, thereby revealing aliphatic carbon functionalities of the starting biomaterials of the mango peel. The  $1422\text{ cm}^{-1}$  absorption band can be ascribed to C=C stretching and C–H bending vibrations, which shows the incomplete graphitization of the carbon material during the process of hydrothermal carbonization. Absorption peaks at  $1163\text{ cm}^{-1}$  and  $1032\text{ cm}^{-1}$  can be associated with C–O and C–O–C stretching vibrations, thereby the presence of alcohol, ether, and ester groups.

The high hydroxyl content and other oxygen-containing functional groups imply high hydrophilicity, thus promoting better dispersion ability in an aqueous environment. But more importantly, these groups function as active sites in adsorption and charge transfer reactions, which promote the degradation process of methylene blue. [2]. The FTIR findings are consistent with those reported for other biomass-derived CQDs, where similar oxygenated surface chemistries have been identified as central to both fluorescence behaviour and photocatalytic activity[60, 61].

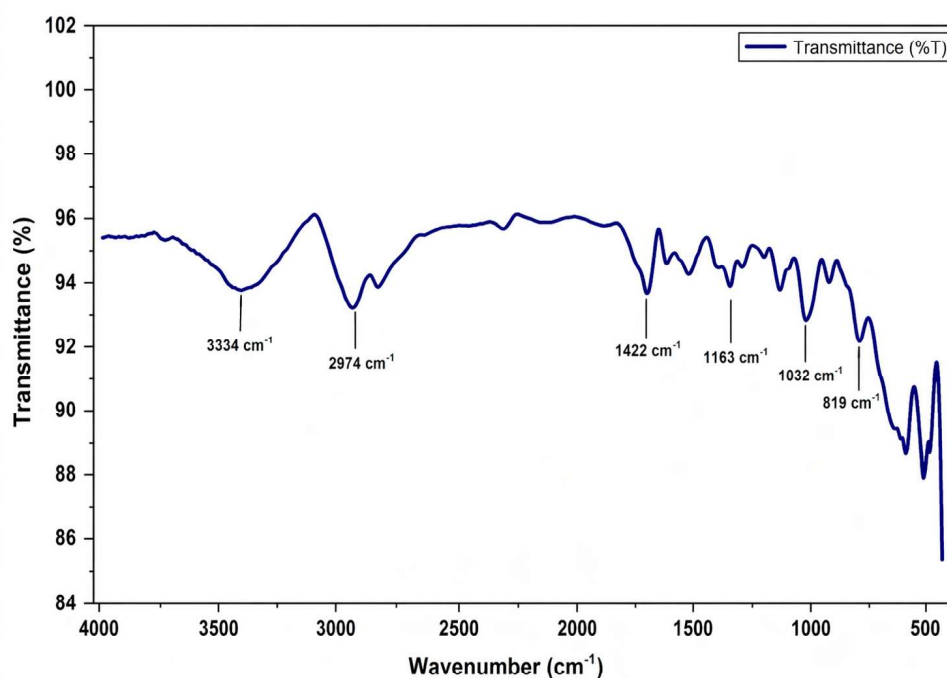


Figure 4.8: FTIR spectrum of carbon quantum dots (CQDs) synthesized from mango peel via hydrothermal treatment.

## 4.6 Adsorption Behavior of Methylene Blue under Dark Conditions

The decrease in absorbance at 664 nm during 90 minutes under dark conditions was used to track the adsorption behavior of methylene blue in the presence of CQDs.  $A_0 = 1.315$  was the starting initial MB absorbance. The absorbance readings and associated degradation efficiencies at each time period are shown in Table 2

Table 4.1: Adsorption Behaviour of Methylene Blue in the Presence of CQDs under Dark Conditions ( $A_0 = 1.315$ ,  $\lambda = 664\text{nm}$ )

Time (min)	Absorbance @ 664nm	Degradation Efficiency(%)
0	1.315	0.00
15	1.285	2.28
30	1.262	4.03
60	1.255	4.56
90	1.252	4.79

Under dark condition, methylene blue absorbance was decreased very slightly, reaching 4.79% at 90 minutes. The decrease in absorbance under dark conditions at 664nm is due to the adsorption of methylene blue onto the surface of CQD. The absorbance drops more quickly in the first stage because there are a lot of active sites on the CQD surface. The active sites ultimately fill up and an adsorption equilibrium is attained is reached, resulting in only a minor additional decline. Due to the lack of light, photocatalytic degradation does not take place.

## 4.7 Photocatalytic Degradation of Methylene Blue under UV Light

The decrease in absorbance at 664 nm during 90 minutes of UV irradiation was used to track the photocatalytic breakdown of MB.  $A_0 = 1.315$  was the starting initial MB absorbance. The absorbance readings and associated degradation efficiencies at each time period are shown in Table 3.

In the UV degradation profile, we can see a clear two-phase pattern. Within the first 0–30 minutes, there was very little degradation (0–5.32%), indicating that methylene blue was mainly adsorbed onto the CQD surface. After 30 minutes, increased photocatalytic degradation boosted their degradation efficiency, which led to a notable increase in degradation between 30 and 60

Table 4.2: Photocatalytic degradation of methylene blue under UV irradiation ( $A_0 = 1.315$ ,  $\lambda = 664\text{nm}$ )

<b>Time (min)</b>	<b>Absorbance @ 664nm</b>	<b>Degradation Efficiency(%)</b>
0	1.315	0.00
15	1.280	2.66
30	1.245	5.32
60	0.820	37.64
90	0.423	67.83



Figure 4.9: Photocatalytic degradation of methylene blue under UV ( $A_0 = 1.315$ ,  $\lambda = 664\text{ nm}$ )

minutes (5.32% to 37.64%). This rise is caused by the generation of reactive species when exposed to UV light. The degradation efficiency, which reached 67.83% after 90 minutes, demonstrated the superior photocatalytic efficacy of CQDs made from mango peels.

The photocatalytic decomposition of methylene blue (MB) using carbon quantum dots (CQDs) under UV light was performed visually and by spectrophotometry at 0, 15, 30, 60, and 90 minutes. The gradual color change in the solution of the dye indicated its successful degradation. As can be seen in Fig ??, the MB solution initially showed a dark navy blue color for  $t = 0$  min with an absorbance of 1.315 at 664 nm wavelength, resulting in a degradation efficiency of 0%. On increasing the time of UV radiation, there was a progressive change in the color of the solution, although it became progressively less intense. The color of the solution at  $t = 15$  min and  $t = 30$  min is mainly that of a dark blue shade, which is related to degradation efficiencies of 2.66% and 5.32% respectively, indicative of an induction period. At the point in time when UV radiation was on for 30 min – 60 min, there was a clear shift in color from a dark to light blue, where the absorbance dropped from 1.245 to 0.820, showing a significant increase in degradation efficiency of 37.64%.

## 4.8 Photocatalytic Degradation of Methylene Blue under Sunlight

For comparison, MB deterioration was assessed while exposed to natural sunshine. Table 4 shows the absorbance and efficiency measurement data recorded under sunlight irradiation.

Table 4.3: Photocatalytic degradation of methylene blue under Sunlight irradiation ( $A_0 = 1.315$ ,  $\lambda = 664 \text{ nm}$ )

Time (min)	Absorbance @ 664nm	Degradation Efficiency(%)
0	1.315	0.00
15	1.250	4.94
30	1.178	10.42
60	1.079	17.95
90	0.962	26.84

Under sunlight irradiation, methylene blue degradation showed a gradual, nearly linear increase, reaching 26.84% at 90 minutes much lower than the 67.83% under UV light. This happens because sunlight includes a lower UV fraction, fluctuating intensity and is less powerful and variable, whereas UV irradiation provides higher and more consistent energy needed for CQD excitation, resulting in larger production of reactive species.

The degradation of methylene blue (MB) was measured in equal time intervals of 0, 15, 30, 60, and 90 minutes, with all other experimental parameters being kept constant as compared to the test using UV light. Figure 4.10 shows that the MB solution maintained its deep navy blue color throughout the entire irradiation duration, with only a slight change in color occurring over 90 minutes. In contrast to the previous UV experiment, there was no noticeable change in color at one particular point in time during irradiation, which can be attributed to the lower energy of photons emitted from the sun compared to those generated using the UV source. Despite that, a small decrease in color still indicated that photocatalysis occurred due to the light absorbing characteristics of the synthesized CQDs.

## 4.9 Comparative Analysis: UV Light versus Sunlight

By directly comparing the two irradiation settings at each time point we can clearly see the improved performance of UV irradiation for CQD-mediated MB photodegradation.

At 15 and 30 minutes, sunlight-exposed samples showed slightly higher degradation than UV

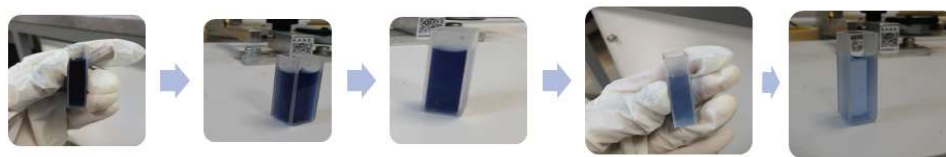


Figure 4.10: Photocatalytic degradation of methylene blue under Sunlight ( $A_0 = 1.315$ ,  $\lambda = 664$  nm)

Table 4.4: Comparative Degradation Efficiency: UV Light vs. Sunlight Irradiation ( $A_0 = 1.315$ ,  $\lambda = 664$  nm)

Time (min)	UV Absorbance	UV Efficiency (%)	Sunlight Absorbance	Sunlight Efficiency (%)
0	1.315	0.00	1.315	0.00
15	1.280	2.66	1.250	4.94
30	1.245	5.32	1.178	10.42
60	0.820	37.64	1.079	17.95
90	0.423	67.83	0.962	26.84

samples due to the initial adsorption-dominant phase under UV conditions. However, from 60 minutes onward, UV irradiation led to significantly higher degradation. By 90 minutes, the UV efficiency (67.83%) was about 2.5 times greater than that under sunlight (26.84%), confirming that UV light is more effective in activating CQDs for methylene blue degradation due to its higher photon energy.

#### 4.10 UV-Vis absorbance spectra of methylene blue (10 mg/L) degradation over time in the presence of mango peel-derived CQDs at $\lambda = 664$ nm

Figure 11 and Figure 12 shown below illustrate the UV-Vis absorption spectra of methylene blue (MB) under UV and solar radiation when carbon quantum dots (CQDs) are present. The distinctive MB absorption peak was seen in both situations about 662-664nm, corresponding to the dye's optical structure. The peak intensity gradually decreased as the irradiation time increased from 15 to 90 minutes, suggesting that methylene blue was continuously degrading. The absorbance at 662 nm dropped from 1.196 to 0.817 under UV illumination, indicating successful dye removal. Similarly but more slowly, the absorbance at 664 nm dropped from 1.226 to 0.974 when exposed to sunlight.

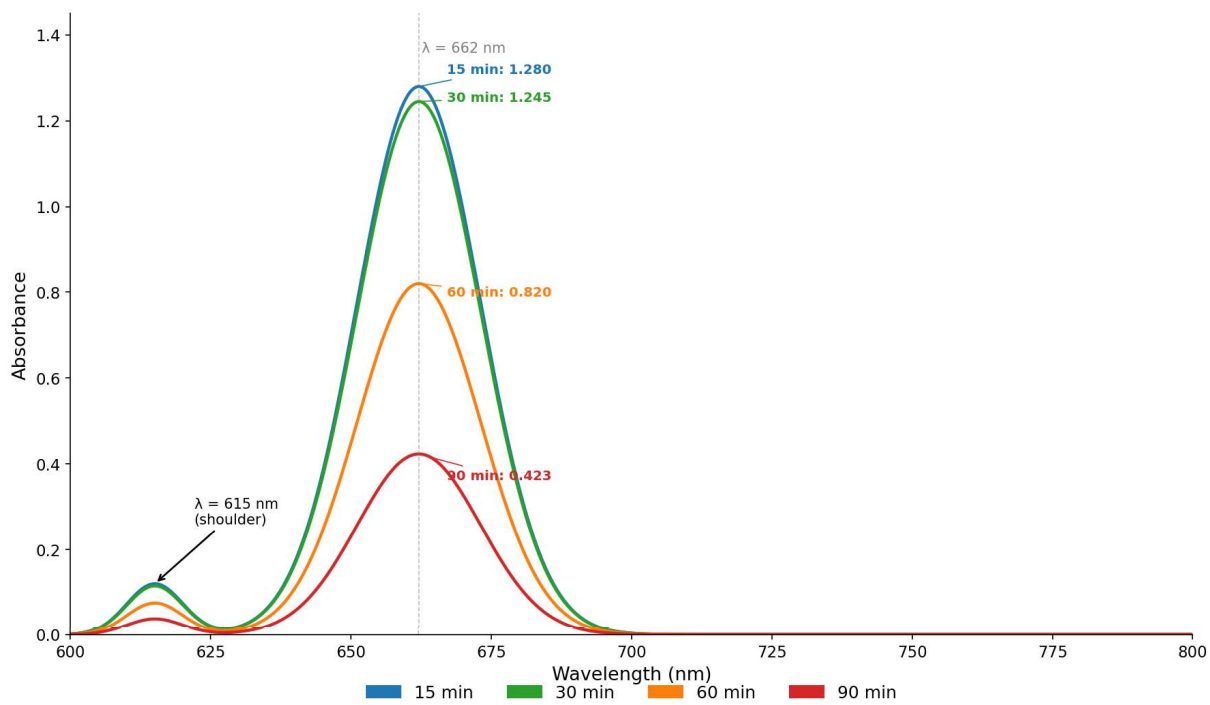


Figure 4.11: (a) UV light

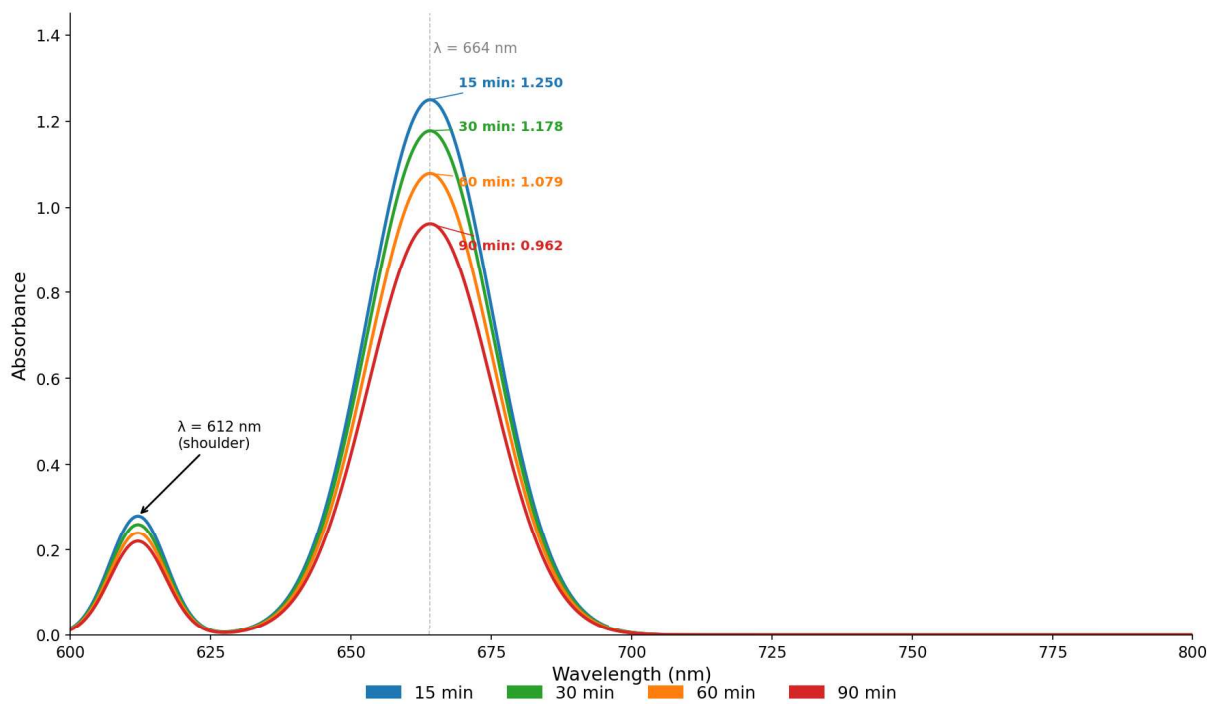


Figure 4.12: (b) Sunlight

## 4.11 Effect of Irradiation Time on Absorbance of Methylene Blue under UV Light and Sunlight

The photocatalytic activity of the produced CQDs was determined using methylene blue in both UV and Sunlight. As the irradiation time increased, the absorbance dropped, indicating dye degradation. After 90 minutes, the absorbance rapidly dropped from 1.315 to 0.423 under UV radiation and from 1.315 to 0.962 under sunlight. Better CQD activation and more reactive species production are indicated by the greater degradation under UV radiation. These findings shows that CQDs made from mango peels are efficient photocatalysts that function better when exposed to UV light.

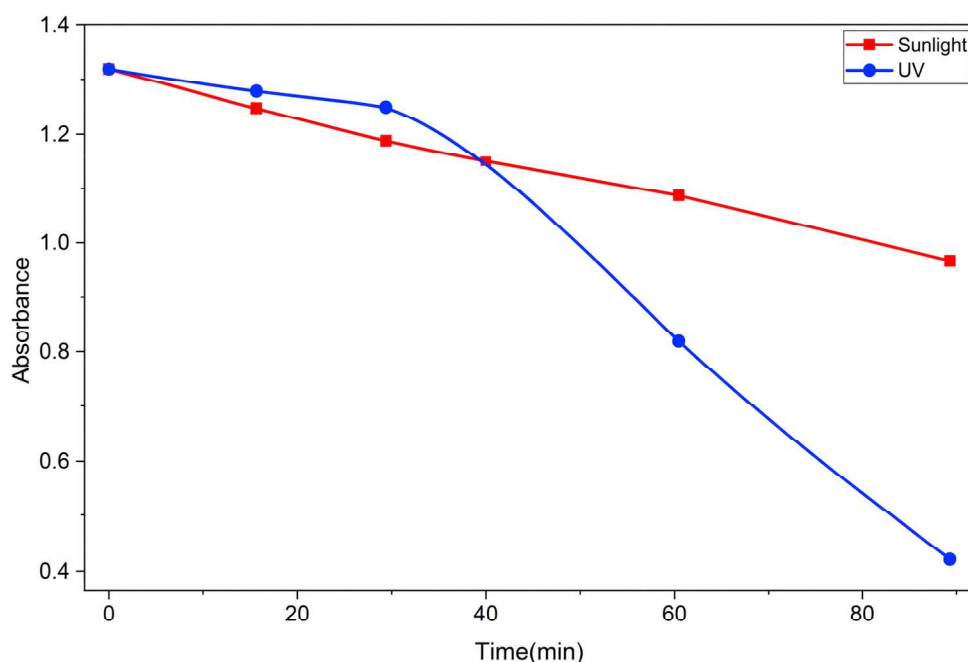


Figure 4.13: Variation of methylene blue absorbance with irradiation time in the presence of CQDs under UV light and sunlight.

## 4.12 Comparative Kinetic Behavior of Methylene Blue Degradation in the Presence of Mango Peel-Derived CQDs under UV Irradiation and Sunlight

Figure 4.14 shows  $\ln\left(\frac{A_0}{A_t}\right)$  vs time to compare the kinetic behaviour of methylene blue degradation in the presence of mango peel derived carbon quantum dot under UV irradiation and sunlight. The  $\ln\left(\frac{A_0}{A_t}\right)$  increased in both cases. The rise was more faster in under UV light than sunlight,

indicating higher photocatalytic activity. After 30 minutes, sunlight developed more slowly and steadily, whereas UV irradiation increased rapidly. This indicates that UV light is more effective at degrading methylene blue and activating CQDs.

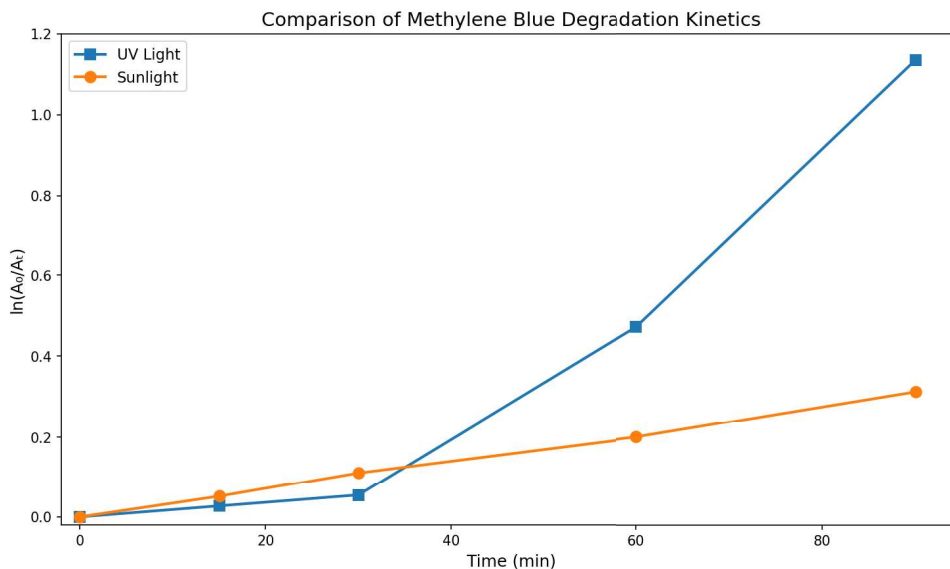


Figure 4.14: Comparison of methylene blue degradation kinetics under UV light and sunlight using  $\ln\left(\frac{A_0}{A_t}\right)$  versus time..

### 4.13 Effect of Irradiation Time on Degradation efficiency of Methylene Blue under UV Light and Sunlight

The degradation efficiency of methylene blue in the presence of carbon quantum dots (CQDs) under UV and solar radiation has been observed. The photocatalytic activity of the produced CQDs was confirmed in both the cases by the steady increase in degradation efficiency with increasing irradiation time. Dye removal significantly improved under UV light, as seen by the degradation efficiency rising from 0% at the beginning to 67.8% after 90 minutes. In contrast, after 90 minutes of exposure to sunlight, the deterioration efficiency only reached 26.8%. This demonstrates clearly that UV light activated the CQD photocatalyst more successfully than sunlight. The decreased deterioration observed during the first phase under UV light may be due to the equilibrium of adsorption between methylene blue molecules and the active surface.

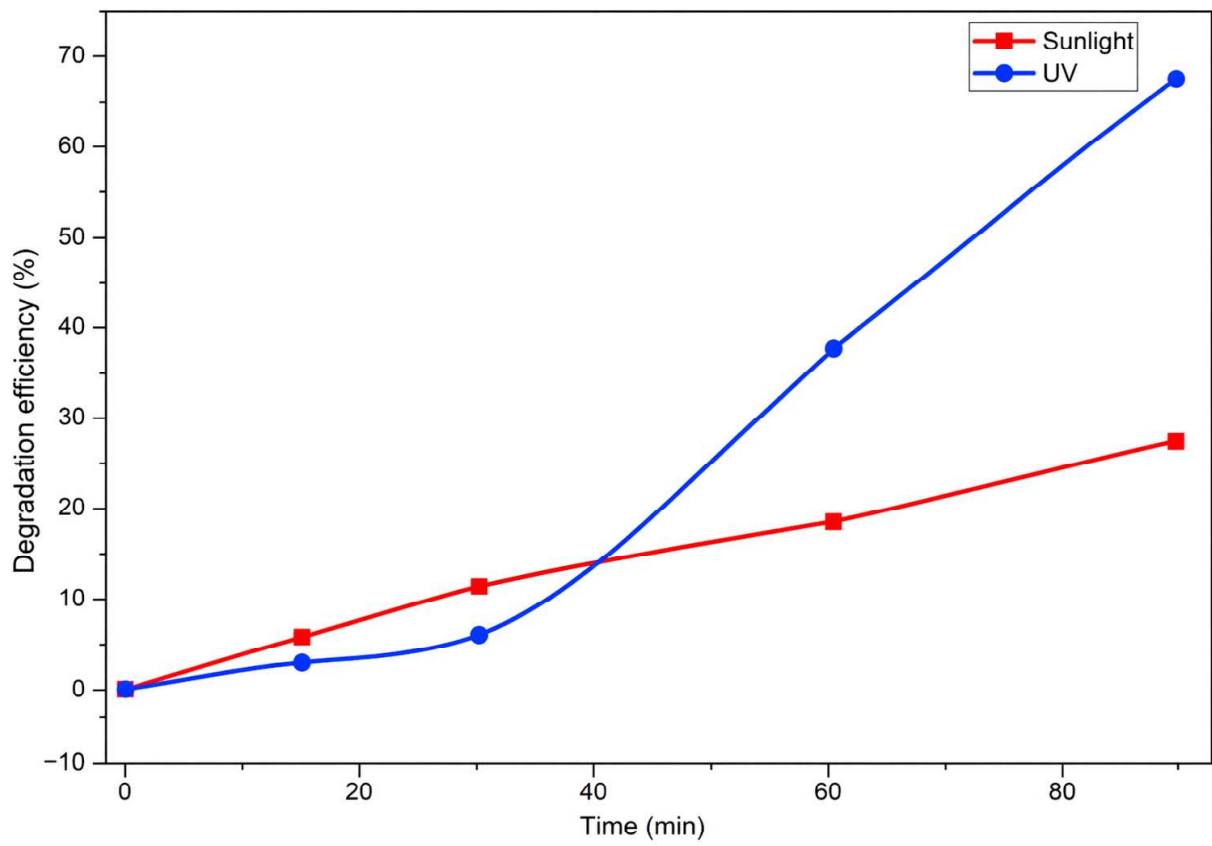


Figure 4.15: Degradation efficiency of methylene blue under UV light and sunlight with irradiation time.

## 5. Conclusion

This study set out to answer a straightforward but meaningful question: can something as ordinary as mango peel waste be transformed into a functional nanomaterial capable of breaking down one of the most common textile dyes found in industrial wastewater? The answer, based on the evidence gathered here, is a clear yes. The synthesis of carbon quantum dots was achieved through a simple, one-step, and eco-friendly hydrothermal method utilizing mango peel waste as precursor material, without the use of any toxic reagent, complicated equipment, or multi-stage synthesis. The resultant CQDs produced were found to be in a stable colloidal state, emitting bright green fluorescence under illumination with 254 nm UV and bright blue under 365 nm. UV-Vis spectrometry showed typical absorbance peaks ranging from 200 to 290 nm, indicative of the presence of an aromatic structure with C=C core and C=O surface groups in the carbon quantum dot structure. Further confirmation of the groups present on the CQD surface was achieved through Fourier transform infrared spectrometry, where hydroxyl, carbonyl, and ether groups were identified. Upon being exposed to methylene blue dye under the action of UV light and natural sunlight, the CQDs showed considerable photocatalytic activities. In the presence of UV light exposure for 90 minutes, the efficiency level stood at 67.83%, an outcome that shows how UV lights enable the efficient excitation of electrons to form oxygen species, which leads to the breaking down of the dye molecules. On the other hand, under natural sunlight exposure, the efficiency level was 26.84% within 90 minutes, an important observation in itself due to the lack of surface modification of the material.

It was discovered through the kinetic study that the degradation process under UV irradiation had a two-step profile, which was the initial step characterized by adsorption within the first 30 minutes and then followed by a rapid rate increase due to photocatalysis, in line with dye degradation via ROS discussed in the general literature. From the findings from the dark adsorption test that recorded a dye removal efficiency of only 4.7%, it can be concluded that photocatalysis and not adsorption is responsible for dye degradation. Collectively, these results strongly support the use of CQDs prepared from mango peels as an environmentally friendly and cost-effective photocatalyst. They are prepared using a waste material, they do not use any harmful chemicals during preparation, they operate efficiently in both UV and sunlight, and they demonstrate efficacy in breaking down an environmental pollutant. From an environmental standpoint, the results reported herein add to the growing literature which demonstrates that what was once considered agricultural waste is now a valuable resource for material science. But there is still much work left to be done. Characterization improvements, optimal synthesis conditions, testing for reuse and application to

other types of pollutants would all make sense for follow-up studies. Yet as a proof-of-concept study, this research has shown that the step from waste to nano-material does not require any chemicals at all—just hot water and a material that would otherwise just end up in the trash.

## 6. Limitations and Future enhancement

### 6.1 Limitations

Every study has some kind of limits I guess, and this one does too. Its important to point out a couple so people dont get the wrong idea about the results.

Mango peel comes from farming stuff, so its not like you can make it all the same every time. The chemicals in it, like those phenolics and sugars, plus how much water is there, they change from one batch to another. Even from one season to the next it varies a lot.

The temperature for the hydrothermal reaction was 130°C, which is below 180°C that is generally considered optimal for full carbonization of biomass [18]. It is likely that since the reaction was conducted below this temperature, the carbonization of the initial material did not occur completely, leading to limited quantum yield.

That could be why the CQDs made ended up with some issues in their fluorescence quantum yield, or at least it seems that way. Not totally sure, but it makes sense.

Characterization of the material was yet another challenge that the research had to overcome. It was not possible to get the exact particle size distribution, crystallinity and zeta potential of CQDs since there was no equipment like TEM or XRD to help do so. This is one of the most basic steps to characterizing these quantum dots.

The sunlight experiment conducted in the outdoors added a certain amount of variability to our results, which was not within our control. The variation in sunlight is not consistent like the artificial light source in a lab, whereby a comparison can be made quantitatively with UV rays.

Finally, the factor of pH was not systematically altered or controlled during all of the photocatalytic experiments. Given that the MB decomposition rate and CQD fluorescence depend on the pH of the solution, this is a factor that should be properly controlled in the future.

### 6.2 Future Enhancement

If this research were to be continued, and we believe it should be, there are several directions that could meaningfully build on what was established here.

However, if such research was to continue which it very much should as there are many different paths that could be followed which could take the research even further. First of all, one of the most logical paths to take would be to develop further the synthesis method used here. By increasing the temperature of the hydrothermal method to reach the vicinity of 180°C and varying the amount of time used for the reactions, the amount of precursor, as well as the pH of the solution, one could

potentially achieve CQDs with better defined structure and fluorescence.

More sophisticated characterization techniques will certainly change what can be said about results such as those found by this study. Using TEM imaging, it would have been possible to view the particles, their sizes, their shapes, and their uniformity. With XRD, the extent of the graphite-like structure of the carbon core could have been established. The zeta potential values would provide information regarding the stability of the CQDs when suspended in solution. Lastly, an accurate measurement of the quantum yield could be achieved. These are just some of the things that were impossible in the study.

Regarding the photocatalytic process, an investigation on the effects of different factors, such as pH, catalyst concentration, dye concentration, and light intensity, on degradation efficiency can be conducted. Currently, only one particular combination of these variables leads to a high level of efficiency. The question is whether there exists some other condition under which efficiency is higher, or whether variations in certain variables have more impact than others.

Another highly promising direction would be to combine the CQDs with hydrogen peroxide ( $H_2O_2$ ) as a co-oxidant in the degradation system. Under light irradiation,  $H_2$  can be decomposed by the CQDs to generate highly reactive hydroxyl radicals ( $\bullet OH$ ), which are among the most powerful oxidizing species known, significantly accelerating the breakdown of dye molecules.

The issue of reusability is yet another critical factor which would need to be examined if this technology is ever to have any practical applications. Testing how the performance of these particles declines after each cycle of degradation would prove very informative. A particle which functions superbly in one application but rapidly loses efficiency thereafter cannot be considered ideal for wastewater treatment purposes.

Later on in the process, nitrogen doping or doping with sulfur or any other heteroatoms is already a proven method for extending the light absorbing properties of CQDs even further into the visible spectrum. And when this can be done using the same concept of going green, then we will have made great strides in making our degradation system highly efficient using just sunlight.

And lastly, methylene blue is a valuable model pollutant; however, there are many more out there. It will be necessary to see how these CQDs behave when exposed to different types of dye and even some medicines as pollutants to gain a better understanding of their full capabilities and to prove that they could be used as an effective photocatalyst in general.

# References

- [1] Kostya S Novoselov, Andre K Geim, Sergei V Morozov, De-eng Jiang, Yanshui Zhang, Sergey V Dubonos, Irina V Grigorieva, and Alexandr A Firsov. Electric field effect in atomically thin carbon films. *science*, 306(5696):666–669, 2004.
- [2] Sheila N Baker and Gary A Baker. Luminescent carbon nanodots: emergent nanolights. *Angewandte Chemie International Edition*, 49(38):6726–6744, 2010.
- [3] Shi Ying Lim, Wei Shen, and Zhiqiang Gao. Carbon quantum dots and their applications. *Chemical Society Reviews*, 44(1):362–381, 2015.
- [4] Haitao Li, Zhenhui Kang, Yang Liu, and Shuit-Tong Lee. Carbon nanodots: synthesis, properties and applications. *Journal of materials chemistry*, 22(46):24230–24253, 2012.
- [5] Dong An, Xianlong Zhang, Fengbing Liang, Mo Xian, Dexin Feng, and Zhiwen Ye. Synthesis, surface properties of glucosyl esters from renewable materials for use as biosurfactants. *Colloids and Surfaces A: Physicochemical and Engineering Aspects*, 577:257–264, 2019.
- [6] Youfu Wang and Aiguo Hu. Carbon quantum dots: synthesis, properties and applications. *Journal of Materials Chemistry C*, 2(34):6921–6939, 2014.
- [7] Jun Zuo, Tao Jiang, Xiaojing Zhao, Xiaohong Xiong, Saijin Xiao, and Zhiqiang Zhu. Preparation and application of fluorescent carbon dots. *Journal of Nanomaterials*, 2015(1):787862, 2015.
- [8] Ya-Ping Sun, Bing Zhou, Yi Lin, Wei Wang, KA Shiral Fernando, Pankaj Pathak, Mohammed Jaouad Meziani, Barbara A Harruff, Xin Wang, Haifang Wang, et al. Quantum-sized carbon dots for bright and colorful photoluminescence. *Journal of the American Chemical Society*, 128(24):7756–7757, 2006.
- [9] Zepeng Qu, Jing Wang, Jianhua Tang, Xiaoqing Shu, Xudong Liu, Zhaohong Zhang, and Jun Wang. Carbon quantum dots/knbo<sub>3</sub> hybrid composites with enhanced visible-light driven photocatalytic activity toward dye waste-water degradation and hydrogen production. *Molecular Catalysis*, 445:1–11, 2018.
- [10] Vinay Sharma, Pranav Tiwari, and Shaikh M Mobin. Sustainable carbon-dots: recent advances in green carbon dots for sensing and bioimaging. *Journal of Materials Chemistry B*, 5(45):8904–8924, 2017.

- [11] R. Khan, S. Shukla, M. Kumar, D. Barceló, A. Zuurro, and P. C. Bhargava. Progress and obstacles in employing carbon quantum dots for sustainable wastewater treatment. *Environmental Research*, 261:119671, 2024.
- [12] P. Li, C. Yang, Z. Jiang, Y. Jin, and W. Wu. Lignocellulose pretreatment by deep eutectic solvents and related technologies: A review. *Journal of Bioresources and Bioproducts*, 8(1):33–44, 2023.
- [13] G. Crini and E. Lichtfouse. Advantages and disadvantages of techniques used for wastewater treatment. *Environmental Chemistry Letters*, 17(1):145–155, 2019.
- [14] Sandeep Sharma and AJAWS Bhattacharya. Drinking water contamination and treatment techniques. *Applied water science*, 7(3):1043–1067, 2017.
- [15] J. Singh, S. Kaur, J. Lee, A. Mehta, S. Kumar, K. H. Kim, and M. Rawat. Highly fluorescent carbon dots derived from mangifera indica leaves for selective detection of metal ions. *Science of the Total Environment*, 720:137604, 2020.
- [16] U. Abd Rani, L. Y. Ng, C. Y. Ng, E. Mahmoudi, Y. S. Ng, and A. W. Mohammad. Sustainable production of nitrogen-doped carbon quantum dots for photocatalytic degradation of methylene blue and malachite green. *Journal of Water Process Engineering*, 40:101816, 2021.
- [17] S. Amloy, T. Lukprang, M. Lertworapreecha, and P. Preechaburana. Green synthesis of carbon dots from mangosteen peel for fluorescent cancer cells. *Journal of Metals, Materials and Minerals*, 34(2):1957, 2024.
- [18] P. V. Duong, M. H. Nguyen, M. H. Do, V. V. Thu, N. D. Dien, D. T. Le, A. T. Le, and T. B. Nguyen. Highly photoluminescent blue-green carbon quantum dots synthesized via plasma solution interaction for bioimaging applications. *Communications in Physics*, 36(1):81–81, 2026.
- [19] R. Khan, S. Shukla, M. Kumar, D. Barceló, A. Zuurro, and P. C. Bhargava. Progress and obstacles in employing carbon quantum dots for sustainable wastewater treatment. *Environmental Research*, 261:119671, 2024.
- [20] H. Salimi Shahraki, R. Bushra, N. Shakeel, A. Ahmad, M. Ahmad, C. Ritzoulis, et al. Papaya peel waste carbon dots/reduced graphene oxide nanocomposite: from photocatalytic decomposition of methylene blue to antimicrobial activity. *Journal of Bioresources and Bioproducts*, 8(2):162–175, 2023.

- [21] D. An, X. Zhang, F. Liang, M. Xian, D. Feng, and Z. Ye. Synthesis, surface properties of glucosyl esters from renewable materials for use as biosurfactants. *Colloids and Surfaces A: Physicochemical and Engineering Aspects*, 577:257–264, 2019.
- [22] M. D. Malitha, M. T. H. Molla, M. A. Bashar, D. Chandra, and M. S. Ahsan. Fabrication of a reusable carbon quantum dots (cqds) modified nanocomposite with enhanced visible light photocatalytic activity. *Scientific Reports*, 14(1):17976, 2024.
- [23] A. M. A. Saputra, A. F. R. Piliang, R. Goei, R. R. HTS, and S. Gea. Synthesis, properties, and utilization of carbon quantum dots as photocatalysts on degradation of organic dyes: A mini review. *Catalysis Communications*, 187:106914, 2024.
- [24] Esther Forgacs, Tibor Cserhádi, and Gyula Oros. Removal of synthetic dyes from wastewaters: a review. *Environment international*, 30(7):953–971, 2004.
- [25] Klaus Hunger. *Industrial dyes: chemistry, properties, applications*. John Wiley & Sons, 2007.
- [26] Mohd Rafatullah, Othman Sulaiman, Rokiah Hashim, and Anees Ahmad. Adsorption of methylene blue on low-cost adsorbents: a review. *Journal of hazardous materials*, 177(1-3):70–80, 2010.
- [27] Mustafa T Yagub, Tushar Kanti Sen, Sharmeen Afroze, and Ha Ming Ang. Dye and its removal from aqueous solution by adsorption: a review. *Advances in colloid and interface science*, 209:172–184, 2014.
- [28] Tim Robinson, Geoff McMullan, Roger Marchant, and Poonam Nigam. Remediation of dyes in textile effluent: a critical review on current treatment technologies with a proposed alternative. *Bioresource technology*, 77(3):247–255, 2001.
- [29] CI Pearce, JR Lloyd, and JT Guthrie. The removal of colour from textile wastewater using whole bacterial cells: a review. *Dyes and pigments*, 58(3):179–196, 2003.
- [30] Roberto Andreozzi, Vincenzo Caprio, Amedeo Insola, and Raffaele Marotta. Advanced oxidation processes (aop) for water purification and recovery. *Catalysis today*, 53(1):51–59, 1999.
- [31] Hong Miao, Lan Wang, Yan Zhuo, Zinan Zhou, and Xiaoming Yang. Label-free fluorimetric detection of cea using carbon dots derived from tomato juice. *Biosensors and Bioelectronics*, 86:83–89, 2016.

- [32] R. Ye, C. Xiang, J. Lin, Z. Peng, K. Huang, Z. Yan, N. P. Cook, E. L. G. Samuel, C.-C. Hwang, G. Ruan, G. Ceriotti, A.-R. O. Raji, A. A. Marti, and J. M. Tour. Coal as an abundant source of graphene quantum dots. *Nature Communications*, 4:2943, 2013.
- [33] N. Kučuk, M. Primožič, P. Kotnik, Ž. Knez, and M. Leitgeb. Mango peels as an industrial by-product: a sustainable source of compounds with antioxidant, enzymatic, and antimicrobial activity. *Foods*, 13(4):553, 2024.
- [34] S. N. Baker and G. A. Baker. Luminescent carbon nanodots: emergent nanolights. *Angewandte Chemie International Edition*, 49(38):6726–6744, 2010.
- [35] Nor Afiqah Nor Asri, Yap Wing Fen, Nurul Illya Muhamad Fauzi, Nur Aqilah Kamaruzzaman, Rahayu Emilia Mohamed Khaidir, Hazwani Suhaila Hashim, Muhammad Fahmi Anuar, Muhammad Amir Zakwan Mohd Zailani, Ahmad Danish Iskandar Mohd Fadzil, Nur Nadia Amira Mahamad Basari, et al. Mango peels-assisted synthesis of carbon quantum dots for potential optical sensing of diazinon. *Scientific Reports*, 16(1):4341, 2026.
- [36] Xiaoyou Xu, Robert Ray, Yunlong Gu, Harry J Ploehn, Latha Gearheart, Kyle Raker, and Walter A Scrivens. Electrophoretic analysis and purification of fluorescent single-walled carbon nanotube fragments. *Journal of the American Chemical Society*, 126(40):12736–12737, 2004.
- [37] Yongqiang Dong, Hongchang Pang, Hong Bin Yang, Chunxian Guo, Jingwei Shao, Yuwu Chi, Chang Ming Li, and Ting Yu. Carbon-based dots co-doped with nitrogen and sulfur for high quantum yield and excitation-independent emission. *Angewandte Chemie International Edition*, 52(30), 2013.
- [38] Haitao Li, Xiaodie He, Zhenhui Kang, Hui Huang, Yang Liu, Jinglin Liu, Suoyuan Lian, Chi Him A Tsang, Xiaobao Yang, and Shuit-Tong Lee. Water-soluble fluorescent carbon quantum dots and photocatalyst design. *Angewandte Chemie International Edition*, 49(26):4430–4434, 2010.
- [39] Libin Tang, Rongbin Ji, Xiangke Cao, Jingyu Lin, Hongxing Jiang, Xueming Li, Kar Seng Teng, Chi Man Luk, Songjun Zeng, Jianhua Hao, et al. Deep ultraviolet photoluminescence of water-soluble self-passivated graphene quantum dots. *ACS nano*, 6(6):5102–5110, 2012.
- [40] SC Ray, Arindam Saha, Nikhil R Jana, and Rupa Sarkar. Fluorescent carbon nanoparticles: synthesis, characterization, and bioimaging application. *The Journal of Physical Chemistry C*, 113(43):18546–18551, 2009.

- [41] Lei Shi, Jian Hai Yang, Hai Bo Zeng, Yong Mei Chen, Sheng Chun Yang, Chao Wu, Hao Zeng, Osada Yoshihito, and Qiqing Zhang. Carbon dots with high fluorescence quantum yield: the fluorescence originates from organic fluorophores. *Nanoscale*, 8(30):14374–14378, 2016.
- [42] Dan Qu, Min Zheng, Ligong Zhang, Haifeng Zhao, Zhigang Xie, Xiabin Jing, Raid E Haddad, Hongyou Fan, and Zaicheng Sun. Formation mechanism and optimization of highly luminescent n-doped graphene quantum dots. *Scientific reports*, 4(1):5294, 2014.
- [43] C Oliver Kappe. Controlled microwave heating in modern organic synthesis. *Angewandte Chemie International Edition*, 43(46):6250–6284, 2004.
- [44] Laurence Perreux and André Loupy. A tentative rationalization of microwave effects in organic synthesis according to the reaction medium, and mechanistic considerations. *Tetrahedron*, 57(45):9199–9224, 2001.
- [45] Idalia Bilecka and Markus Niederberger. Microwave chemistry for inorganic nanomaterials synthesis. *Nanoscale*, 2(8):1358–1374, 2010.
- [46] Yoonsang Park, Yujin Kim, Heemin Chang, Sungyeon Won, Hyemin Kim, and Woosung Kwon. Biocompatible nitrogen-doped carbon dots: synthesis, characterization, and application. *Journal of Materials Chemistry B*, 8(39):8935–8951, 2020.
- [47] Xin-Yue Jiao, Lu-shuang Li, Si Qin, Yu Zhang, Kun Huang, and Li Xu. The synthesis of fluorescent carbon dots from mango peel and their multiple applications. *Colloids and Surfaces A: Physicochemical and Engineering Aspects*, 577:306–314, 2019.
- [48] Jagpreet Singh, Sukhmeen Kaur, Jechan Lee, Akansha Mehta, Sanjeev Kumar, Ki-Hyun Kim, Soumen Basu, and Mohit Rawat. Highly fluorescent carbon dots derived from mangifera indica leaves for selective detection of metal ions. *Science of the Total Environment*, 720:137604, 2020.
- [49] Md Dipu Malitha, Md Tamzid Hossain Molla, Md Abul Bashar, Dipesh Chandra, and Md Shameem Ahsan. Fabrication of a reusable carbon quantum dots (cqds) modified nanocomposite with enhanced visible light photocatalytic activity. *Scientific Reports*, 14(1):17976, 2024.
- [50] Hela Ferjani, Sahar Abdalla, Opeyemi A Oyewo, and Damian C Onwudiwe. Facile synthesis of carbon dots by the hydrothermal carbonization of avocado peels and evaluation of the photocatalytic property. *Inorganic Chemistry Communications*, 160:111866, 2024.

- [51] Gouri Sankar Das, Jong Pil Shim, Amit Bhatnagar, Kumud Malika Tripathi, and TaeYoung Kim. Biomass-derived carbon quantum dots for visible-light-induced photocatalysis and label-free detection of Fe (iii) and ascorbic acid. *Scientific reports*, 9(1):15084, 2019.
- [52] Phm Văn Dng, Minh Hoa Nguyen, Minh Hieu Do, Vu Van Thu, Nguyen Dac Dien, Duc Toan Le, Anh Thi Le, and Thanh Binh Nguyen. Highly photoluminescent blue–green carbon quantum dots synthesized via plasma solution interaction for bioimaging applications. *Communications in Physics*, 36(1):81–81, 2026.
- [53] RM Silverstein, FX Webster, DJ Kiemle, and DL Bryce. Spectrometric identification of organic compounds, eighth edition, John Wiley & Sons. Inc., NJ, 2014.
- [54] Hesam Salimi Shahraki, Rani Bushra, Nimra Shakeel, Anees Ahmad, Mehraj Ahmad, Christos Ritzoulis, et al. Papaya peel waste carbon dots/reduced graphene oxide nanocomposite: from photocatalytic decomposition of methylene blue to antimicrobial activity. *Journal of Bioresources and Bioproducts*, 8(2):162–175, 2023.
- [55] Maribel García-Mahecha, Herlinda Soto-Valdez, Elizabeth Carvajal-Millan, Tomás Jesús Madera-Santana, María Guadalupe Lomelí-Ramírez, and Citlali Colín-Chávez. Bioactive compounds in extracts from the agro-industrial waste of mango. *Molecules*, 28(1):458, 2023.
- [56] N Matinise, N Botha, A Fall, and M Maaza. Enhanced photocatalytic degradation of methylene blue using zinc vanadate nanomaterials with structural and electrochemical properties. *Scientific Reports*, 15(1):26333, 2025.
- [57] Yaoyao Yang, Kangliang Peng, Yakun Deng, Youjun Zhao, Jinshui Ai, Xiao Min, Mengzhu Hu, Shuai Huang, and Lixin Yu. Full-color-emission carbon quantum dots by controlling surface states in a system of solvent. *Journal of Luminescence*, 243:118614, 2022.
- [58] Y. Wang and A. Hu. Carbon quantum dots: synthesis, properties and applications. *Journal of Materials Chemistry C*, 2(34):6921–6939, 2014.
- [59] Jichuan Kong, Yihui Wei, Feng Zhou, Liting Shi, Shuangjie Zhao, Mengyun Wan, and Xiangfeng Zhang. Carbon quantum dots: properties, preparation, and applications. *Molecules*, 29(9):2002, 2024.
- [60] Velu Manikandan and Nae Yoon Lee. Green synthesis of carbon quantum dots and their environmental applications. *Environmental research*, 212:113283, 2022.
- [61] A Muhammad Afdhal Saputra, Averroes Fazlur Rahman Piliang, Ronn Goei, Risky Ramadhan HTS, Saharman Gea, et al. Synthesis, properties, and utilization of carbon quantum dots as

photocatalysts on degradation of organic dyes: A mini review. *Catalysis Communications*, 187:106914, 2024.

# Appendices

## Appendix A: Raw Experimental Data

### A.1 Dark Adsorption Data

Table 6.1: Raw absorbance data for MB adsorption under dark conditions ( $A_0 = 1.315$ ,  $\lambda = 664$  nm)

Time (min)	Absorbance @ 664 nm	Degradation Efficiency (%)
0	1.315	0.00
15	1.285	2.28
30	1.262	4.03
60	1.255	4.56
90	1.252	4.79

### A.2 UV Irradiation Degradation Data

Table 6.2: Raw absorbance data for MB degradation under UV irradiation ( $A_0 = 1.315$ ,  $\lambda = 664$  nm)

Time (min)	Absorbance @ 664 nm	Degradation Efficiency (%)
0	1.315	0.00
15	1.280	2.66
30	1.245	5.32
60	0.820	37.64
90	0.423	67.83

### A.3 Sunlight Irradiation Degradation Data

Table 6.3: Raw absorbance data for MB degradation under sunlight ( $A_0 = 1.315$ ,  $\lambda = 664$  nm)

Time (min)	Absorbance @ 664 nm	Degradation Efficiency (%)
0	1.315	0.00
15	1.250	4.94
30	1.178	10.42
60	1.079	17.95
90	0.962	26.84

### Appendix B: UV-Vis Spectral Peak Summary

Table 6.4: Summary of UV-Vis spectral features of CQDs under different solvent conditions

Sample	Peak Wavelength (nm)	Max Absorbance	UV Range at 280 nm
Normal (Undiluted)	200–280	0.435	0.339
Ethanol-Diluted	280	0.825	0.825
Distilled Water-Diluted	200	0.882	0.552

The undiluted sample showed the weakest and broadest absorption, consistent with higher particle concentration causing scattering effects. The ethanol-diluted sample produced the sharpest and most resolved peaks, indicating better particle dispersion. The distilled water-diluted sample showed the highest overall absorbance, attributed to the greater exposure of oxygen-containing surface functional groups in the polar aqueous medium.

### Appendix C: FTIR Peak Assignments

Table 6.5: FTIR absorption peaks and their assignments for mango peel-derived CQDs

Wavenumber ( $\text{cm}^{-1}$ )	Assignment	Functional Group
3334	O–H stretching vibration	Hydroxyl group (–OH), adsorbed moisture
2974	C–H stretching vibration	Aliphatic carbon structures
1422	C=C stretching / C–H bending	Partially graphitized carbon domains
1163	C–O stretching	Alcohol, ether, ester groups
1032	C–O–C stretching	Ether linkages
819	C–H out-of-plane bending	Aromatic C–H

The presence of these functional groups confirms that the synthesized CQDs possess a hydrophilic,

oxygen-rich surface that facilitates both aqueous dispersibility and photocatalytic activity through adsorption and charge transfer mechanisms.

## Appendix D: Sample Degradation Efficiency Calculation

The photocatalytic degradation efficiency ( $\eta$ ) was calculated using the following expression:

$$\eta (\%) = \frac{A_0 - A_t}{A_0} \times 100 \quad (6.1)$$

where  $A_0$  is the initial absorbance of MB at 664 nm and  $A_t$  is the absorbance at irradiation time  $t$ .

### Example 1: UV Irradiation at $t = 90$ min

$$A_0 = 1.315$$

$$A_{90} = 0.423$$

$$\eta = \frac{1.315 - 0.423}{1.315} \times 100$$

$$\eta = \frac{0.892}{1.315} \times 100$$

$$\eta = \mathbf{67.83\%}$$

### Example 2: Sunlight Irradiation at $t = 90$ min

$$A_0 = 1.315$$

$$A_{90} = 0.962$$

$$\eta = \frac{1.315 - 0.962}{1.315} \times 100$$

$$\eta = \frac{0.353}{1.315} \times 100$$

$$\eta = \mathbf{26.84\%}$$

### Example 3: Dark Conditions at $t = 90$ min

$$A_0 = 1.315$$

$$A_{90} = 1.252$$

$$\eta = \frac{1.315 - 1.252}{1.315} \times 100$$

$$\eta = \frac{0.063}{1.315} \times 100$$

$$\eta = \mathbf{4.79\%}$$

## Appendix E: Kinetic Analysis Data

The pseudo-first-order kinetic parameter  $\ln\left(\frac{A_0}{A_t}\right)$  was calculated at each time point for both UV and sunlight conditions and used to generate the kinetic plots in Figure 4.12.

Table 6.6: Calculated  $\ln(A_0/A_t)$  values for MB degradation under UV and sunlight

<b>Time (min)</b>	<b>UV <math>A_t</math></b>	<b>UV <math>\ln(A_0/A_t)</math></b>	<b>Sunlight <math>A_t</math></b>	<b>Sunlight <math>\ln(A_0/A_t)</math></b>
0	1.315	0.000	1.315	0.000
15	1.280	0.027	1.250	0.051
30	1.245	0.054	1.178	0.110
60	0.820	0.473	1.079	0.198
90	0.423	1.135	0.962	0.312

The steeper rise in  $\ln(A_0/A_t)$  under UV irradiation compared to sunlight confirms a higher apparent rate constant under UV, consistent with more efficient CQD excitation and greater reactive oxygen species generation under UV photons.



त्रिभुवन विश्वविद्यालय  
TRIBHUVAN UNIVERSITY  
इन्जिनियरिङ्ग अध्ययन संस्थान  
INSTITUTE OF ENGINEERING

पुल्चोक क्याम्पस  
PULCHOWK CAMPUS



5-521260  
5-521611  
5-522104  
5-522809

Accredited by University Grants  
Commission (UGC) Nepal 2020

पुल्चोक, ललितपुर।  
Pulchowk, Lalitpur



Date: May 8, 2026

To Whom It May Concern:

This is to certify that the paper titled "*Hydrothermal Synthesis of Carbon Quantum Dots from Mango Peel Waste and Their Application in Photocatalytic Degradation of Methylene Blue*" (Submission ID #1069), with **Nikita Shrestha** as the first author, was accepted through the peer-review process and has been presented at the 18<sup>th</sup> IOE Graduate Conference, organized at Pulchowk Campus, Lalitpur, Nepal, from May 7 to 9, 2026.

Please note that inclusion of the accepted manuscript in the conference proceedings is contingent upon timely compliance with any further editorial requirements during the publication process.

Prof. Sangeeta Singh  
Convener  
18<sup>th</sup> IOE Graduate Conference





# IOE Graduate Conference

## Certificate of Participation



This certificate is awarded to

*Nikita Shrestha*

in recognition of an invaluable contribution to  
the academic discourse and research dissemination  
at the 18<sup>th</sup> IOE Graduate Conference held from May 7 to 9, 2026  
organized by Pulchowk Campus, Lalitpur, Nepal  
through the **Paper Presentation** entitled

*"Hydrothermal Synthesis of Carbon Quantum Dots from Mango Peel Waste and their Application  
in Photocatalytic Degradation of Methylene Blue."*

Prof. Sangeeta Singh  
Conference Convener

Prof. Sanjay Uprety  
Champus Chief, Pulchowk Campus

Prof. Sushil Bahadur Bajracharya  
Dean, Institute of Engineering